DOE/NASA/51040-27
NASA TM-82620

Test Results and Facility Description for a 40-Kilowatt Stirling Engine

Gary G. Kelm, James E. Cairelli,
and Robert J. Walter
National Aeronautics and Space Administration
Lewis Research Center

June 1981

Prepared for
U.S. DEPARTMENT OF ENERGY
Conservation and Renewable Energy
Office of Vehicle and Engine R&D

DOE/NASA/51040-27
NASA TM-82620

Test Results and Facility Description for a 40-Kilowatt Stirling Engine

Gary G. Kelm, James E. Cairelli,
and Robert J. Walter
National Aeronautics and Space Administration
Lewis Research Center
Cleveland, Ohio 44135

June 1981

Work performed for
U.S. DEPARTMENT OF ENERGY
Conservation and Renewable Energy
Office of Vehicle and Engine R&D
Washington, D.C. 20545
Under Interagency Agreement DE-AI01-77CS51040

TEST RESULTS AND FACILITY DESCRIPTION FOR A 40-KILOWATT STIRLING ENGINE

Gary G. Kelm, James E. Cairelli, and Robert J. Walter

National Aeronautics and Space Administration
Lewis Research Center
Cleveland, Ohio 44135

SUMMARY

NASA Lewis Research Center is conducting tests with a 40-kilowatt, P40 Stirling engine manufactured by United Stirling of Malmö, Sweden. This experimental research is part of a project sponsored by the Department of Energy (DOE) to develop an automotive Stirling engine propulsion system. The overall project goal is to demonstrate by September 1984 the potential advantages this alternative engine offers for powering highway vehicles (e.g., high fuel economy, multifuel capability, low noise, and emissions).

The P40 was designed by United Stirling to be a reliable "workhorse" engine for testing and developing specific components (e.g., the heater head, piston rod seals, and piston rings). Because it was intended as a rugged experimental engine, the P40 is too heavy to be a practical automotive Stirling engine. Nevertheless, it was selected as the project's "baseline" engine because it was an available, convenient starting point from which to derive Stirling engine operating experience. Consequently, while the "MOD I" automotive Stirling engine is being designed and built for the project, several P40 engines are being evaluated in test cells and in vehicles by organizations involved in the development effort.

NASA P40 tests are being conducted (1) to establish the engine's baseline performance and emissions characteristics for comparison with other engines, (2) to provide data for validating computer models, (3) to identify problem areas which must be addressed in future Stirling engine designs, and (4) to evaluate the performance of advanced systems or components installed in the engine.

This report focuses on the NASA P40 engine testing activity which began in April 1979. Included is a description of the P40 engine along with its control systems and auxiliaries. Also described are the engine test support facilities, instrumentation, data acquisition systems, and experimental procedures. Finally, engine operating experience is discussed, and some initial test results are presented.

INTRODUCTION

The Stirling engine was invented in 1816 by Robert Stirling, a Scottish minister. From a chronological perspective, this makes the Stirling engine a relatively old concept. It was conceived in the days before Carnot and Joule and predates many better-known devices such as the electric motor and the steam, diesel, and Otto-cycle engines. In spite of its chronological age, however, the Stirling engine is relatively immature in terms of its technological development. While modern heat engines have been actively developed for many years by numerous organizations, the Stirling engine has remained in relative obscurity. Over the last 20 years, several companies have conducted modest efforts to develop the Stirling engine; but most of

these efforts can be traced to the N. V. Philips Company of The Netherlands. Philips began the development of high-specific-power Stirling engines in 1937 and was the principal modern developer of Stirling engine technology until the corporate decision was made in 1980 to withdraw from active Stirling engine development. Much progress has been made; however, very few modern Stirling engines have been produced to date.

There are a wide variety of potentially promising commercial applications for Stirling engines. These range from driving heat pumps for home heating and cooling to propelling highway vehicles and even to powering implantable artificial hearts. The Stirling engine could also be used in various mining, marine, construction, and industrial applications (e.g., for powering compressors or electrical generating sets) and can produce electricity or pump water in remote areas using focused solar energy.

There are several important reasons why the Stirling engine appears to be attractive in so many different applications. Among them are its high efficiency, multifuel capability, low noise, and low emissions. With these characteristics, and its other advantages, the external combustion Stirling engine offers potential as a possible alternative to the internal combustion Otto (gasoline) and diesel engines for powering highway vehicles. (See ref. 1 for a description of automotive Stirling engine pros and cons.) However, although the automotive application provides a very large market for heat engines, it also places severe demands on their performance, durability, and cost. Consequently, the relatively underdeveloped Stirling engine, despite its potential advantages, is not currently in a position to compete with the well-established and proven technology of the internal combustion engine.

There are several factors that have restricted development of the Stirling engine for automotive or other applications. These include its higher cost and complexity and its unproven reliability. These problems are typified by the engine's need for better seals and lower-cost heat exchanger materials. Perhaps an even more important obstacle to Stirling engine development involves the fact that many potential manufacturers already have a very large capital investment in the existing technology of internal combustion engines. These manufacturers would have to be convinced that an alternative engine could succeed economically as well as technically before they would invest very heavily in its development.

Based on legislation from Congress, the U.S. Department of Energy (DOE), in an effort to stimulate possible commercial production of advanced heat engines, established a Government-funded program to promote their development. The near-term program objective is to demonstrate the advantages of these alternative engines in highway vehicle applications.

Within the DOE program is a project managed by the NASA Lewis Research Center to develop an advanced automotive Stirling engine. Information about this project can be found in references 2 to 5. Work in the project is being carried out primarily by a contract team comprising Mechanical Technology Incorporated (MTI), United Stirling of Sweden, and AM General (AMG), a subsidiary of American Motors Corp. A limited amount of work is also being conducted in-house at NASA Lewis.

This report describes part of Lewis' in-house Stirling activity, specifically that involving tests with a P40 Stirling engine built by United Stirling of Sweden. It is intended to lay the ground-work for future reports on P40 engine experiments by providing background information about the P40 engine, our test support facilities, and our experimental pro-

cedures. The report also includes a discussion of our operating experience with the engine and presents some initial test results.

OBJECTIVES

NASA P40 engine tests are being conducted primarily to support the DOE automotive Stirling engine development effort. However, some tests are also being carried out as part of a project funded by the Bureau of Mines to evaluate alternative engines for mining applications and particularly to assess the emissions characteristics of the Stirling engine.

Objectives of the DOE-funded tests are to (1) characterize the P40's baseline performance and emissions with engine-driven auxiliaries, (2) provide experimental data for validating Stirling engine computer codes, (3) evaluate the in-engine performance of advanced components which look promising in rig tests or offer the potential for lower manufacturing costs, and (4) gain operating experience to identify design weaknesses and to enhance NASA's capability to independently evaluate and direct future development of automotive Stirling engines.

Bureau of Mines tests are intended to (1) evaluate engine exhaust emissions with diesel fuel, (2) evaluate engine performance with helium working gas, and (3) assess engine reliability and durability in mining application duty cycles.

APPARATUS AND PROCEDURE

P40 Engine Description

Basic engine. - The P40 is a four-cylinder, double-acting Stirling engine built by United Stirling of Malmo, Sweden. Some of the design and performance characteristics of the P40 are summarized in table I. Additional information about the engine can be found in references 6 to 10. Figure 1 is a cross section of the P40, and figure 2 shows photographs of the engine installed in a NASA test cell.

The P40 is designed to produce 40 kilowatts of power at 4000 rpm using hydrogen working gas at 15 megapascals mean cycle pressure with an average heater-tube wall temperature of 720° C and a cooling-water inlet temperature of 50° C. Power output of the engine is controlled by varying the mean cycle pressure while maintaining a nearly constant heater-tube wall temperature.

There are four major sections of the engine (see fig. 1): (1) the preheater/combustor, (2) the heater head assembly, (3) the cylinder block, and (4) the crankcase. Each section of the engine will now be described.

The preheater/combustor is part of the engine's external heating system, which also includes air-fuel and heater temperature control systems, which will be discussed later. The overall function of the external heating system is to make heat available to the engine's closed cycle working gas (i.e., hydrogen or helium). To accomplish this, combustion air at near-atmospheric pressure is forced by a blower through the recuperative air preheater. The preheater (fig. 3) is essentially a counterflow heat exchanger which contains an annular matrix comprising a large number of thin, corrugated stainless-steel plates. The plates are seam welded in pairs to form separate flow paths such that combustion air passing up through the matrix is preheated by outgoing exhaust gases without mixing the two flows. The preheated air passes through a turbulator which swirls the air as it enters

the combustor and mixes with fuel and atomizing air injected from a nozzle (see fig. 4). The mixture is ignited by a continuously operating, electrically energized ignitor located near the nozzle. The resulting hot combustion gases transfer required heat to the engine as they pass over two rows of heater tubes before they travel down through the preheater matrix and leave the engine from dual exhaust ports. It is interesting to note that if the preheater/combustor assembly were removed and the heater head modified, it would still be possible to operate the engine using another source of available heat (e.g., focused solar energy or heat pipes drawing heat from thermal storage).

The P40's heater-head assembly is divided into four, separable quadrants. Figure 5 shows photographs of the heater-head assembly (a), an individual heater quadrant (b), and the heater quadrant components (c). Each quadrant is composed of 18 heater tubes and 3 castings. Two castings house the regenerators, while the third forms the upper section of the cylinder. Two concentric heater-tube rows are formed by bending the tubes and brazing the ends into manifolds, which are part of the castings. The inner row of tubes is bent in an involute shape in such a way that the entire tube assembly forms a conical surface that is sealed to the combustor at the outer edge (see fig. 1). The outer row consists of straight, vertical, finned tubes which form a cylindrical surface when the four heater quadrants are installed on the engine.

When the heater-head assembly is bolted to the cylinder block, the castings in each quadrant become part of the cylinder and regenerator-cooler pressure vessels. The cylinders, which enclose the reciprocating pistons, are oriented in a so-called "square-four" arrangement when viewed from above (see fig. 1). The eight regenerator-cooler pressure vessels (two per cycle) also form a square that surrounds the cylinders. The regenerators (see figs. 5(c) and 6) are made by sintering stacks of stainless-steel screens of a specific wire diameter and mesh size. This method of fabrication is rather expensive, but it does result in highly effective heat transfer between the working gas and the regenerator material. The gas coolers (see figs. 5(c) and 7) are installed directly below the regenerators and extend into the cylinder block. The coolers are sealed at their regenerator interface and in the block with O-ring seals to prevent working gas from escaping into the cooling water. The coolers are fabricated in a single-pass tube-and-shell configuration using bundles of small diameter tubes through which the working gas passes. Heat is rejected to cooling water which circulates around the tubes in a single crossflow arrangement.

The cylinder block (see fig. 8) is made using nodular cast iron. Into the block are cast the cylinders, water jackets, and cooler-flow plate housings. The aluminum flow plates (figs. 5(c) and 8) direct the flow of working gas between the coolers and the engine's compression spaces. Circulating cooling water is directed into the center of the block from which it is radially distributed through the jackets to abstract heat from the cylinders and cycle coolers. Water flows in four parallel paths, passing through two coolers in series before exiting through two outlet passages on opposite sides of the block.

The piston assembly comprises a piston base and piston dome (fig. 9). The piston base contains machined grooves for the piston rings and guide rings which are made from Rulon LD, a polytetrafluoroethylene (PTFE)-based material. When the engine operates, the piston rings run dry against the cylinder walls, since lubricating oil in the cylinders would contaminate the regenerators and adversely affect engine performance. The drilled holes in

the piston base are part of a system to improve piston ring life by maintaining minimum engine cycle pressure between the rings, thereby reducing axial ring motion in the grooves. When a piston is installed in the engine, the base is pressed onto the tapered piston rod (see fig. 10), and the dome is then screwed into the threaded rod end. The dome interior volume is vented to the space between the piston rings and, by the check valve action of the rings, is maintained at minimum engine cycle pressure. An O-ring (shown in fig. 9) seals the dome against the base and isolates the dome volume from fluctuating cylinder pressures.

The lower part of the cylinder block is machined to accommodate the piston rod seal housings (see fig. 11(a)). The seals in these housings (fig. 11(b)) are designed to prevent the oil in the crankcase from migrating into the cylinders and, at the same time, to prevent high-pressure working gas from leaking into the crankcase. The seal housings also contain the crosshead bearing surfaces which aline the piston rods to the high-pressure rod seals. Good alinement is necessary for the seals to work properly as reciprocating piston motion is transmitted to the crank shafts through the connecting rods. Other surfaces of the cylinder block are machined to create the required interfaces, including the upper face, upon which the heater-head assembly is mounted and sealed.

The lower face of the cylinder block interfaces with the crankcase, which contains the P40's mechanical drive unit. This unit was designed for United Stirling by Ricardo Consulting Engineers of England.

Figure 10 shows the piston rod, crosshead, and connecting rod assemblies which drive two separate crankshafts. The crankshafts are geared to a common power output drive shaft. The crankcase also houses the required shaft bearings and a chain-driven lubrication-oil pump for the drive unit components. The crankcase is closed but not tightly sealed, and its pressure remains near atmospheric pressure during engine operation.

Control systems. - A simplified diagram of the P40 power control system is shown in figure 12. Key to the system is an electrohydraulic servovalve which controls the flow of hydrogen working gas to and from the engine.

The valve has four functional positions: supply, neutral, dump, and dump/short-circuit. When the accelerator is depressed, demanding an increase in engine power, the servovalve moves to the supply position and allows hydrogen to flow from the storage bottle to the engine's cylinders, raising the mean cycle pressure. At cruise the valve moves to the neutral position, and the engine's mean cycle pressure remains constant. To decelerate, the servovalve moves to the dump or dump/short-circuit position. In dump the engine power is gradually reduced as hydrogen is pumped to the storage bottle by means of a double-acting, engine-driven hydrogen compressor. Dump/short-circuit provides a very rapid power decrease by interconnecting the engine's cylinders to absorb energy by circulating working gas between the working spaces while hydrogen is pumped to the storage bottle.

The P40's temperature and air-fuel control systems are shown schematically in figure 13. The temperature control system is designed to maintain constant heater tube wall temperature over all engine operating conditions to insure that engine performance is acceptable and that heater-head life is not adversely compromised. The air-fuel control system is designed to regulate the air-fuel ratio for proper combustion system performance and low exhaust emissions.

Combustion air is supplied to the engine by a regenerative blower driven by the engine through a variable-ratio belt drive. An air throttle downstream of the blower regulates the airflow rate to the preheater/com-

bustor. The position of the air throttle is adjusted by an electric servomotor, which responds to signals from control thermocouples measuring heater tube wall temperature. When the heater-tube temperature drops, the control thermocouples sense an engine demand for heat, and the control system causes the air throttle to open so more air flows to the preheater/combustor. When the heater-tube temperature exceeds the temperature control set point, the air throttle moves toward the closed position, reducing air flow to the preheater/combustor. Excess air from the blower is recirculated to the blower inlet by means of a bypass built into the air throttle valve. To reduce NO_x emissions, some exhaust gases are also recirculated, passing through an exhaust-gas recirculation (EGR) flow-control valve before mixing with combustion air in the blower bypass line.

The EGR valve (see fig. 14) contains two ports: The small port opens by means of a temperature-sensitive bimetal lever; the large port is opened with a position-adjustable solenoid. The small port opening depends only on exhaust temperature; so, once the external heating system warms up, a small amount of exhaust gas will continuously be recirculated. However, most EGR flow passes through the large port. A solenoid controls the opening and closing of this port, while an externally adjustable stop regulates the amount of open area. Solenoid operation depends on a flow switch in the combustion-air system. At near-idle conditions, when airflow is low, the switch keeps the solenoid-controlled port closed, since little EGR is needed. At higher power conditions, larger quantities of exhaust gas must be recirculated to maintain low NO_x levels. Consequently, as power and airflow increase, the flow switch opens the solenoid port to provide more EGR.

While airflow is governed by a temperature-controlled air throttle valve, fuel flow is regulated by a modified Bosch K-Jetronic air-fuel ratio controller (see fig. 13). This unit senses the airflow by means of a plate in the inlet air stream. The plate is mechanically linked to a valve in the fuel line. As the plate moves in response to changes in airflow rate, the fuel valve moves as well, so that the desired air-fuel ratio is always maintained. An electric fuel pump and associated valving maintains constant fuel pressure while the system operates and returns excess fuel to the fuel tank. For a given fuel-control pressure, air-fuel ratio depends solely on the position of the airflow sensor plate which, in turn, depends on the contour of the air funnel. Some adjustment in air-fuel ratio is possible by changing fuel control pressure with the pressure regulating valve.

Electronics. - The P40 makes use of a solid-state, linear, analog electronic system to provide all necessary engine control functions. (The required electronic equipment was supplied to us by United Stirling as part of the hardware delivered with the engine.) The power and temperature control systems described previously depend on the engine electronics for their logic and proper operation. The power control system in particular relies on predetermined, empirically derived relationships programmed into the controller to produce the desired engine torque-speed characteristic. Control system electronics also provide over a dozen separate abort functions for engine protection and contain the engine start-stop sequences shown in table II.

The P40 control panel (see fig. 15) incorporates the engine function commands (i.e., start, stop, fuel cutoff, emergency gas dump, and accelerator), panel meters to monitor critical engine parameters (e.g., speed, oil and cooling water temperature, working gas pressure, etc.), and potentiometers to simulate engine signals during prerun checkout of the start-stop

sequences and the abort functions. Lights are also provided on the panel to indicate the status of the engine and the abort system.

Auxiliaries. - For automotive or other applications requiring "self-contained" engine operation, a Stirling engine must include a number of auxiliaries. (A distinction should be made between engine auxiliaries, which encompass devices that are required for "self-contained" operation, and engine accessories, which include devices for passenger comfort, safety, or convenience such as an air conditioning compressor or power steering pump.)

Listed below are descriptions of the auxiliaries installed on the P40 in tests being conducted at NASA. A radiator fan and electric aftercooling pump are the main auxiliaries missing from the list that would be required in an automotive installation. Figure 16 is a plot provided by United Stirling that shows the calculated power consumption of some of the engine auxiliaries.

Combustion air blower: The combustion air blower used in this installation is a rather inefficient (37 percent maximum efficiency) regenerative device, driven by the engine through a variable ratio belt drive. This drive is centrifugally actuated to reduce blower power consumption at higher engine speeds. An electrically operated air throttle valve located downstream of the blower is used to control airflow rate to the preheater/combustor as part of the heater-head temperature control system described previously.

Atomizing air compressor: The atomizing air compressor is a belt-driven, carbon vane, positive-displacement device which provides pressurized air for fuel atomization at the fuel nozzle. A pressure-regulating valve limits atomizing air pressure, and a bypass line recirculates excess air to the compressor inlet.

Alternator: A standard automotive-type alternator rated at 14 volts, 55 amperes is belt-driven by the engine. As the P40 operates the alternator recharges the two storage batteries, one of which is used for control system electronics and the other for engine startup power requirements.

Hydraulic oil pump: The hydraulic oil pump is a gear-type pump driven by the engine through the variable-ratio belt drive. The pump charges an accumulator, which maintains oil pressure in the hydraulic system by means of a nitrogen overpressure. Hydraulic oil is used to operate valves in the engine's power control system, including the electrohydraulic servovalve.

Hydrogen compressor: The hydrogen compressor (see fig. 12) is driven directly by the engine from an eccentric on one of the crankshafts. When engine power output is to be reduced or the engine shut down, the hydrogen compressor pumps working gas from the engine's cylinders to a hydrogen storage reservoir, as discussed previously. The compressor is double-acting, thus providing hydrogen compression in both directions of piston travel. When the compressor is not required, it is externally short-circuited through a solenoid valve to reduce the power consumed.

Cooling water pump: The cooling water pump is a centrifugal device which is belt-driven by the engine. The pump circulates water through the cooling jacket of the hydrogen compressor and across the tubes of the eight cycle-gas coolers in order to transfer rejected heat from the engine to a radiator or other external heat exchanger to be dissipated to the atmosphere.

Lubrication oil pump: The lubrication oil pump is a gear-type pump driven by means of a sprocket-chain drive from one of the engine's crankshafts. The pump circulates engine oil (SAE 20W40) from the crankcase through an oil filter to areas requiring lubrication, such as piston rods

and seals, crossheads, bearings, and gears. A pressure relief valve in the oil system limits the maximum supply pressure, and a thermostat regulates oil temperature by diverting oil flow to a cooler.

Auxiliaries startup motor: The auxiliaries startup electric motor is used during the automatic start sequence to drive the combustion air blower, atomizing air compressor, and hydraulic oil pump. The motor is a permanent magnet type rated as 12 volts and 500 watts.

Engine starter motor: The P40 starter motor is a conventional automotive engine starter rated at 12 volts, 1.9 kilowatts. The starter engages gear teeth in the engine flywheel and cranks the engine during the automatic starting sequence once the heater temperature has reached about 600° C.

DESCRIPTION OF FACILITY SYSTEMS

Dynamometer tests with the P40 have been carried out thus far with the engine in a "self-contained" configuration, where auxiliaries are driven by the engine as they would be in an automotive installation. Several additional systems have been provided in the test cell to support research and operational requirements and to insure safety in case of failure. These systems are shown schematically in figure 17 and are described below.

Engine Cooling Water Temperature Control System

The power and efficiency of a Stirling engine are strongly influenced by the temperatures of its heater head and cycle cooler. A temperature control system, described previously, maintains constant heater-head temperature. To maintain constant cooler temperature, the radiator and cooling fan used for the automotive installation were replaced by a closed-loop cooling-water-temperature control system. The basic elements of this system include the engine-driven water pump, an external, motor-driven water pump (to improve cooling at low engine speeds and after the engine is shut down), a three-way, closed-loop temperature-control valve, an expansion tank, and a heat exchanger to transfer engine-rejected heat from the closed-loop system to cooling tower water. The closed-loop system contains approximately 60 liters of demineralized water treated with sodium dichromate to form a 500 ppm solution, which inhibits oxidation and corrosion of engine parts.

Engine Lubrication Oil Cooling System

Heat rejected to the engine's lubricating oil is dissipated by a separate oil cooler installed in the test-cell basement. In the cooler, heat from the circulating oil is transferred to cooling tower water which serves as a secondary coolant heat sink. In addition to the oil cooler, the lubrication system includes the previously discussed engine-driven oil pump, filter, relief valve, and thermostat. Oil temperature into the engine normally ranges from about 55° to 85° C, depending on engine speed and load.

Dynamometer and Dynamometer Cooling System

An Eaton universal eddy-current dynamometer (model B-20U rated at 93 kW) is used to measure and absorb engine power. The dynamometer has both speed and torque control capabilities. To date, only the speed control mode of operation has been used. The dynamometer also has a 15-kilowatt motoring capability.

The dynamometer cooling system is independent of the engine cooling system. Dynamometer heat absorbed by the system is transferred to cooling tower water through a heat exchanger.

Fuel Supply System

The fuel supply system comprises two, removable, 208-liter storage barrels and a fuel pump located outside the test cell, a 19-liter, gravity-feed tank located inside the cell, along with an electrically operated fuel pump, filter, flowmeter, and associated valves and tubing. Before testing the engine, fuel is pumped to the in-cell tank from outdoor fuel storage. To date the primary fuel used for P40 tests has been Indolene (an unleaded test gasoline marketed by the American Oil Company), though diesel fuel has also been used for some engine tests.

During engine operation, fuel is supplied by gravity from the in-cell tank to the fuel pump. Fuel flow to the fuel nozzle is regulated by the Bosch K-Jetronic air-fuel ratio controller. Two independently operated solenoid valves (one controlled by engine electronics, the other by test cell systems) are located in series near the fuel nozzle, so fuel supply to the combustor can be cut off immediately in the event of a temperature control malfunction, fire, or other emergency.

Test Cell Ventilation and Safety Systems

Two potentially dangerous fluids are used in P40 testing: fuel for combustion (e.g., Indolene or diesel fuel) and the closed-cycle working gas, hydrogen (though the inert gas helium is used instead of hydrogen for some engine tests). In the interest of safety special precautions are taken and detailed procedures are followed in operating the engine. In addition, the test cell is ventilated with a 4700 liter-per-second capacity exhaust fan to prevent the accumulation of combustible fuel vapors and to promote the rapid diffusion of hydrogen in the event of a major leak. Make-up air is drawn from an outside air supply duct, and the ventilation rate provides a complete test cell air change about once every 45 seconds. Should the ventilation system fail, an alarm sounds, and the fuel valve is automatically closed.

Detectors are installed in the test cell to sense the presence of hydrocarbons (fuel vapor), hydrogen, heat, and smoke. If any of these detectors are activated, an alarm sounds in the control room and at the Center's fire station to alert safety personnel of a fire or potential fire. Should a fire occur in the test cell, a Cardox (carbon dioxide) system can be manually activated to flood the cell with CO_2. Activating the CO_2 system also sounds an alarm at the fire station and in the control room to alert personnel in the vicinity of the danger.

Dry nitrogen gas is available in the test cell so the combustor can be remotely purged in an emergency. Nitrogen is also used as a purge gas as part of the crankcase ventilation system. In this system a continuous flow of low pressure nitrogen passes through the crankcase to carry away any hydrogen that might leak past the piston rod seals. A vent line from the crankcase discharges the purge gas outside the test cell.

Hydrogen/Helium Supply System

In an automotive Stirling engine installation, the hydrogen storage reservoir located in the engine compartment functions as part of the mean pressure power control system. The reservoir must periodically be recharged, since hydrogen may be gradually lost from the closed system due to seal leakage and diffusion through high-temperature heater tubes.

In the test cell the 7-liter reservoir supplied with the engine for use in P40 automotive installations has been retained. In addition a separate supply system has been provided to charge the reservoir and engine with either hydrogen or helium working gas. A 42-liter bottle of hydrogen or helium (pressurized to about 15 MPa) is installed in the test cell before an engine test. Hand valves are positioned to supply the engine and reservoir with the desired working gas. If hydrogen is to be used, the engine is first purged with nitrogen or helium to insure that no oxygen is present when the hydrogen is introduced. Subsequent pressure-vent purge cycles are then performed with hydrogen.

A system is available to obtain small samples of engine working gas before or after a test. These samples later may be analyzed by mass spectroscopy to determine their composition. The analysis can reveal if pretest purging was inadequate or if the working gas was contaminated in some way as a result of operating the engine (e.g., leakage of lube oil into the working space can cause a buildup methane gas and carbon which would degrade engine performance).

Exhaust System

Exhaust gases from the P40 combustor are vented to the outside atmosphere through an exhaust system installed in the test cell. The system includes two flexible exhaust lines and an exhaust stack. The lines connect to the two P40 preheater exhaust outlets and join at a Y-connection in the exhaust stack. The stack contains the EGR valve, described previously, which returns some exhaust gas to the combustor in order to reduce combustion flame temperature and thereby limit formation of nitrogen oxides (NO_x).

Samples of exhaust gas are taken at several locations in the combustion system (see fig 8). A vacuum pump and solenoid valves are used to direct gases from a particular location in the combustion system to an exhaust gas analyzer system. The analyzer system (see fig. 19) contains instruments to measure the emission levels of the following exhaust gas constituents: carbon monoxide, carbon dioxide, nitrogen oxides, total hydrocarbons, and oxygen.

Instrumentation

As furnished by United Stirling, the P40 contained the instrumentation needed to safely operate and control the engine. Figure 15 shows the control panel delivered with the engine, and table III lists the engine and control system parameters measured by United Stirling-supplied instrumentation.

As tests with the engine have proceeded, we have gradually added more instrumentation when convenient to do so (e.g., during engine overhauls). For backup and comparison purposes, a few of the measurements we have added duplicate those made by United Stirling's instrumentation. However, most of

The new instrumentation has expanded our measurement capabilities to previously unmeasured parameters. An overall summary of currently installed instrumentation is provided in table IV.

Part of the instrumentation we have added is intended for measuring the engine's indicated power (or indicated mean effective pressure - IMEP) based on pressure-volume diagrams from the expansion and compression spaces. Figure 20 shows some of the electronic hardware associated with this IMEP measurement system. In a future report we plan to describe this system in some detail and present the experimental results obtained.

Data Acquisition Systems

Steady-state, digital (ESCORT). - A minicomputer-based digital data recording and display system known as Escort is used in P40 testing. The system is intended primarily for steady-state data recording; however, its high sampling rate (≈5000 samples/sec) allows us to acquire multiple scans for each data point recorded. (We normally record 5 to 10 scans taken over a period of about 15 to 30 sec.) The scans are averaged, and statistical information is calculated to indicate the extent to which measured parameters vary.

The Escort system has many on-line features and capabilities. It can convert and display in real time the values of all measured parameters in engineering units as well as in millivolts. It can perform on-line calculations and present the results on constantly updated LED and selectable CRT displays, from which hard copy printouts can be obtained on a local typewriter terminal. It can limit-check measured and calculated values and automatically initiate a warning or predetermined action should a limit be exceeded. Escort also contains a "history file" feature which enables one to "freeze" the minicomputer's recent memory of acquired data (recorded at ≈2-sec intervals) and examine these data on-line almost immediately. This provides a powerful tool for analyzing engine failures or examining relatively slow transients. (The interested reader may consult ref. 11 for a much more comprehensive description of the Escort system.)

Transient analog. - To acquire transient data from the P40 engine, an analog recording system is available. This system includes a 14-track high-speed, FM tape recorder with multiplexing capability to permit continuous recording of up to 150 separate data channels. Data recorded on tape must subsequently be processed to be analyzed. Selected channels can, for example, be output to a strip-chart recorder or be digitized and batch processed on a digital computer.

Data are normally recorded at a tape speed of about 3 meters per second; however, lines to the remotely located analog recorder limit the system's frequency response to approximately 10 kilohertz, which is sufficient for most of our transient measurement requirements. For greater response a separate recorder must be installed in our control room.

Data Taking Procedure

To reduce the chances of taking invalid data, a standard procedure is used to set steady-state engine test conditions. Initially, the engine is started by means of the automatic start sequence regulated by the P40 electronic control system. The engine is allowed to warm up until oil and cooling water temperatures have stabilized. The repeatability of engine performance is checked by comparing on-line data with data recorded previously

under the same test conditions. Provided no significant change is observed, testing proceeds.

Test conditions are generally set by fixing mean cycle pressure and heater/cooler temperatures and then adjusting engine speed to the desired level using the dynamometer speed control. It normally takes about 30 minutes for all engine temperatures to stabilize after a cold start, and about 10 to 15 minutes are needed for stabilization between test conditions.

When emissions data are taken, data points are normally recorded from each of the five emissions sampling stations (see fig. 18) while the engine operates at a fixed test condition (i.e., fixed pressure, speed, and heater/cooler temperatures). The sampling stations are selected in the same order for each test condition. When a particular sampling station has been selected by opening the appropriate solenoid valve, some time must be allowed for the gas sample to reach the analyzers and for the measurements to stabilize. Experience has shown this time to be about 30 to 40 seconds for our system. Consequently, it takes about 5 to 6 minutes to acquire data from all five sampling stations, including about 30 seconds to record each data point. To insure accurate emissions measurements, all analyzer calibrations are checked while waiting for the engine temperatures to stabilize between test conditions by using calibration gases of known concentration.

RESULTS AND DISCUSSION

Operating History

One objective in P40 testing is to identify problems that must be addressed in future Stirling engine designs. Operating experience can provide an indication of the reliability of various engine components and systems and pinpoint design weaknesses.

Figure 21 shows the operating history of P40 engine number 1 since testing began at NASA in April 1979. The failures experienced are identified by symbols defined in the key. The failures listed include facility problems as well as several minor, one-of-a-kind engine problems. Two types of repetitive engine failures have been encountered: those involving check valves in the mean pressure control system and those involving O-rings. The failures directly or indirectly attributable to check valves or O-rings are separately identified in the figure.

Direct check-valve failures have not occurred since United Stirling provided us with new-style check valves, model Hawe ER-2, which replaced the original, model Hawe RC-2 valves (fig. 22). O-ring failures would appear likely to occur in the P40 if only because of the large number of O-rings used in the design to facilitate the numerous rebuilds normally expected with a development engine. A few of the O-ring failures we experienced probably occurred because the O-rings had not been properly installed in "blind" assemblies.

The most significant other failures experienced in the course of P40 testing have involved the piston-rod seals and the engine heater head. The rod seals originally installed in the P40 were Leningrader-type sliding seals. Figure 23 shows an assembly stackup of this rod seal arrangement, which includes a hydrogen seal, a rod scraper, and a cap seal. The Leningrader configuration did not prove effective in preventing oil from entering the cycle and contaminating the regenerators and other heat exchangers. Consequently, the original Leningrader seal was replaced by the pumping Leningrader (PL) seal, recently developed by United Stirling. The PL

rod seal stackup was shown in figure 11(b). United Stirling has successfully operated the PL rod seals in test engines for several thousand hours. Our first experience with them was not nearly so successful; however, we believe the failure which occurred may have resulted from a rod and seal misalinement that occurred during installation. A second set of PL seals has been installed and appears to be functioning very well after more than 100 hours of operation in the engine.

An instrumented P40 heater-head quadrant is shown in figure 24. The heater-head quadrant failure we experienced involved a small leak in a brazed joint between a heater tube and one of the regenerator housing manifolds. To repair this leak, several tube fins had to be removed (see fig. 25(a)).

The leak area was repair brazed using Nioro braze (82 percent Au, 18 percent Ni) alloy with localized electron-beam heating. A ceramic cement was then used to fill the void left by the removed fins (see fig. 25(b)). Based on leak tests and engine operation after the repair brazing, it appeared that the repair procedure was successful. However, a second leak developed after about 109 hours of operation (including about 4 hr at 820° C heater-head temperature). This leak was quite small and, upon inspection, was found to be caused by a small porosity in the heater tube itself just above the repair brazed area. The porosity perhaps resulted from a local stress concentration due to the original repair braze or due to increased thermal stress caused by blocking off the repaired area with ceramic material. The tube was repaired using the same brazing procedure, but this time the quadrant was reinstalled without filling the finless repaired area with ceramic cement (see fig. 25(a)). No further leaks have developed in the limited amount of testing done since this most recent repair.

All problems experienced with the P40 are documented on failure or discrepancy notices. These notices are issued for each of the P40 engines being tested as part of the project, and they are distributed on a regular basis to all project participants (i.e., NASA, MTI, United Stirling, and AMG). This system of exchanging information enables us to identify common P40 problems and possibly prevent their future occurrence in P40 engines. The recent hardware modifications implemented based on testing experience should improve P40 reliability and lead to a longer mean time between failures for the MOD I engines.

Data

Figures 26 to 29 present measured engine performance results for the engine operating with hydrogen and/or helium working gas. With the exception of figure 29, all performance data were taken with an average measured heater tube wall temperature of 720° C and a cooling water inlet temperature of 50° C.

Figures 26(a) and (b) show engine power and torque as functions of engine speed for various mean working pressures of hydrogen, the gas for which the P40 was designed. (Data were not taken at high-pressure, low-speed conditions because of bearing design limitations.) As would be expected, the figures show that power and torque increase as the mean working gas pressure increases. This occurs because a larger mass of working gas is available in the cycle at higher pressures, producing greater forces on the engine pistons. For a fixed pressure, power tends to increase almost linearly with speed up to about 2500 rpm; however, as engine speed is increased further, the rate of power increase is reduced because of higher mechanical friction

and larger aerodynamic flow losses through the heat exchangers. Torque curves are relatively flat with speed; but for a fixed pressure, peak torque tends to occur at minimum engine speed. This is desirable since high torque at low speed improves vehicle acceleration characteristics or lugging capability and can simplify transmission requirements. Like the steam engine and series-wound electric motor, the Stirling engine offers power-torque characteristics which, for vehicle applications, are superior to those offered by the internal combustion engine.

Figure 26(c) presents a map of brake specific fuel consumption (BSFC) as a function of engine power for various speeds and hydrogen working gas pressures, with heat to the engine provided by combustion of Indolene fuel. Minimum BSFC shown (about 314 g/kW-hr) corresponds to a brake thermal efficiency (BTE) of about 26.5 percent and occurs at 15 megapascals mean working pressure, 2000 rpm engine speed, and a power level of approximately 25 kilowatts. It should be noted that BSFC and BTE are based on fuel flow and, consequently, include losses associated with the engine's external heating system. If these losses were removed, BTE would be greater than 30 percent for the minimum BSFC condition cited above. At a fixed pressure minimum BSFC (or maximum efficiency) occurs at some intermediate speed between 1000 and 4000 rpm (i.e., ≈2000 rpm). This occurs because of the influence of flow losses and conduction losses. As discussed previously, flow losses tend to restrict the rate of power increase at higher engine speeds, and, consequently, reduce engine efficiency at these speeds.. On the other hand, at lower engine speeds conduction losses become a significant percentage of the heat input, which thereby also reduces engine efficiency.

Just as power and torque increase with increasing levels of pressure, efficiency also increases (i.e., BSFC decreases) with higher pressures for a fixed speed or power level. However, the relative gain in power, torque, and especially efficiency decreases as pressure increases for a fixed speed. This can be attributed, at least in part, to heat-transfer limitations in the engine. As pressure increases, a larger mass of working gas must be alternately heated and cooled in the cycle. Consequently, even though the heater-tube temperature and cooling-water-inlet temperature are held constant, the working-gas temperatures vary with engine pressure. As pressure is increased for a fixed speed, compression space gas temperatures increase while expansion space gas temperatures decrease. (A similar gas temperature effect occurs when engine speed is increased at fixed pressure, because of the increased heat flux at higher power.) As a result of these engine heat-transfer limitations, Carnot efficiency based on gas temperature is lower at higher engine pressures and speeds in spite of holding heater tube and cooling-water temperature constant.

Figure 27 corresponds to figure 26 and illustrates how the engine performs with helium as its working gas instead of hydrogen. Figure 27(a) shows engine power versus speed with mean working-gas pressure as a parameter. These curves are similar to the hydrogen power curves (fig. 26(a)) in their tendency to increase linearly at lower engine speeds. However, unlike hydrogen, the helium curves peak at around 3000 rpm and decrease dramatically at higher engine speeds because of the larger flow losses with helium.

The P40's helium torque-speed characteristics are shown in figure 27(b) for various levels of mean working-gas pressure. Like hydrogen, the helium torque curves are highest at minimum engine speed. However, because of the larger helium flow losses, the curves are steeper than the corresponding hydrogen torque curves (fig. 26(b)).

Figure 27(c) presents a BSFC versus power performance map for various helium working-gas pressures and engine speeds for the engine operating with Indolene. Minimum BSFC (≈360 g/kW-hr) corresponds to a brake thermal efficiency of about 24 percent and occurs at 15 megapascals mean working pressure, 1500 rpm engine speed, and about a 16-kilowatt power level. Removing external heating system losses increases BTE to about 28 percent at minimum BSFC.

Figure 28 directly compares engine performance with hydrogen and helium using a plot of power versus speed for three different levels of engine mean cycle pressure. The curves plotted were also used in figures 26(a) and 27(a). Figure 28 clearly illustrates the high-speed performance penalties associated with switching to helium but also shows that penalties are greatly reduced at lower engine speeds. At speeds above 3000 rpm, for example, power is down by as much as 50 to 60 percent when the engine uses helium instead of hydrogen; however, at speeds below 2000 rpm, power is down only about 10 to 20 percent. Based on these results, it does not seem unreasonable to speculate that had the P40 been designed for helium rather than hydrogen, its low-speed performance might be essentially equal for the two gases.

Figure 29 shows the effect of increased heater-tube wall temperature on engine power and efficiency for a range of speeds when the engine operates using hydrogen at the maximum mean cycle pressure of 15 megapascals. Maximum power at 790° C was about 41 kilowatts as compared with about 36 kilowatts at 720° C, while maximum efficiency at 790° C was about 27.5 percent as compared with about 26.5 percent at 720° C for an engine speed of 2000 rpm. A more detailed investigation into the engine's performance sensitivity to various heater-cooler temperature combinations will be presented in a future report.

Also shown in figure 29 for comparison are some data generated by United Stirling during P40 engine number 1 acceptance tests in Sweden. (Note that the 4000-rpm acceptance test point was taken at a cooling-water inlet temperature of 60° C.) We believe that most of the performance differences we have observed in comparing our results with those from the acceptance tests can be attributed to differences in heater head operating temperature test conditions.

For NASA tests we try to maintain a constant measured average heater-tube wall temperature (nominally 720° C) which is based on signals from 16 thermocouples evenly spaced around the circumference of the heater head. Twelve of these thermocouples are attached to rear-row heater tubes, while the remaining four thermocouples are attached to front-row tubes. All wall temperature thermocouples are located on the so-called "shady" side of the heater tube, opposite the flow of combustion gases.

When tests began with P40 number 1, our heater-tube wall temperature measurements were unreliable because of the method used to install the thermocouples. The thermocouples were mechanically attached to the heater tubes by inserting them in wells (attached to the tubes) while all four heater-head quadrants were being assembled to the engine. During this installation procedure, it was not possible to insure that all the thermocouples remained in their wells and made good contact with the tube walls. Furthermore, dislodged thermocouples could not be identified until the engine was tested. During a cold engine startup, dislodged thermocouples tended to respond more quickly; and during steady-state engine operation, they read high, tending to indicate a combustion-gas temperature rather than a tube wall temperature. Because we could not be certain of good tube wall contact, question-

able thermocouple measurements were removed from our calculation of the average tube wall temperature.

To improve the reliability of wall temperature measurements, we developed another method of attaching thermocouples to the heater tubes. Our method relied on tack welding the thermocouples to the tubes, making the thermocouples a permanent part of each heater-head quadrant. Short leads from the tube thermocouples terminate in quick-disconnect connectors that can easily be separated when the heater head is disassembled.

Based on our experience with this alternative installation, we believe our heater-tube thermocouples are now providing more reliable wall-temperature measurements since the likelihood of good tube wall contact has been improved. However, we still have some uncertainty about the absolute significance of these measurements. To increase our understanding, we have installed thermocouples to measure gas temperatures in the engine's expansion spaces. We have also added other instrumentation (see table IV) that will help us evaluate more-detailed aspects of engine and combustion system performance.

CONCLUDING REMARKS

This report is primarily intended to provide background information and lay the groundwork for future reports concerning tests with the United Stirling P40 engine. After experiencing many early problems, the engine is currently performing well. We believe the hardware changes that were implemented (e.g., switching to improved check valves and piston rod seals) have increased the engine's reliability. We also believe engine performance is as expected if apparent differences in heater-head operating temperature test conditions are taken into consideration. Based on United Stirling's experience with more than 20 P40 engines they have built, it appears that engine performance is normally repeatable and engine-to-engine performance differences are likely to be relatively small.

REFERENCES

1. Martini, W. R.: International Developments in Stirling Engines. Fifth International Symposium on Automotive Propulsion Systems, Department of Energy, CONF-800419, Vol. 1, 1980, pp. 369-390.
2. Ragsdale, R. G.: Stirling Engine Project Status. Proceedings of the Highway Vehicle Systems Contractors' Coordination Meeting, Department of Energy, CONF-781050, 1979, pp. 287-291.
3. Beremand, Don G.: Stirling Engines for Automobiles. NASA TM-79222, 1979.
4. Aronson, Robert B.: Stirling Engine - Can Money Make it Work? Mach. Des., vol. 52, no. 9, 1980, pp. 20-27.
5. Automotive Stirling Engine Development Program. Quarterly Technical Progress Reports (Mechanical Technology, Inc.; NASA Contract DEC 3-32):
   Allen, M., ed.: MTI81ASE163QT10, NASA CR-165194, 1980.
   Allen, M., ed.: MTI80ASE144QT9, NASA CR-165134, 1980.
   Allen, M., ed.: MTI80ASE129QT8, NASA CR-159851, 1980.
   Allen, M., ed.: MTI80ASE116QT7, NASA CR-159827, 1980.
   Derikart, T. A.; and Allen, M.: MTI79ASE101QT6, NASA CR-159744, 1980.
   Derikart, T. A.; and Allen, M.: MTI79ASE88QT5, NASA CR-159610, 1979.
   Zerucka, T. A.; and Allen, M.: MTI79ASE67QT4, NASA CR-159606, 1979.

6. Rosenqvist, Kaj; and Haland, Yngve: United Stirling's P-40 Engine - Three Years' Experience of Testing, Evaluation, and Improvements. Fifth International Symposium on Automotive Propulsion Systems, Department of Energy, CONF-800419, Vol. 1, 1980, pp. 336-355.
7. Slaby, Jack G.: Overview of a Stirling Engine Test Project. Fifth International Symposium on Automotive Propulsion Systems, Department of Energy, CONF-800419, Vol. 1, 1980, pp. 285-303.
8. Bratt, Christer: Design Characteristics and Test Results of the United Stirling P40 Engine. Energy to the 21st Century; Proceedings of the 15th Intersociety Energy Conversion Engineering Conference, American Institute of Aeronautics and Astronautics, Inc., 1980, Vol. 3, pp. 1964-1966.
9. Rosenqvist, N. K. G.; and Sjostedt, L. E.: The Stirling Engine as a Candidate for Automotive Prime Movers. Institution of Mechanical Engineers (London), Conference Publ. No. 1979-13, 1979, pp. 79-94.
10. Kelm, Gary G.; and Cairelli, James E.; P40 Stirling Engine Number 1 Test Results and Operating Experience at NASA. Presented at the Automotive Technology Development Contractor Coordination Meeting, Nov. 11-13, 1980.
11. Miller, Robert L.: Escort: A Data Acquisition and Display System to Support Research Testing. NASA TM-78909, 1978.

TABLE I. - P40 STIRLING ENGINE DESIGN/PERFORMANCE CHARACTERISTICS

Overall dimensions, mm	785x655x580
Dry weight (including auxiliaries), kg	329
Brake power[a] at 4000 rpm, kW	≈40
Brake thermal efficiency[a] at 2000 rpm, percent	≈29
Working gas	hydrogen
Working gas mass[b], g	<100
Number of cylinders	4 (square 4 arrangement)
Displacement, l	0.38
Bore, mm	55
Stroke, mm	40
Drive	dual crank, crankshafts geared to driveshaft
Method of power control	mean cycle pressure modulation (15 MPa, max)
Fuel	unleaded regular gasoline or diesel fuel
Range of air-fuel ratio[c]	15 to 25
Heater type	involute tubular
Number of tubes	72
Number of tubes per quadrant	18
Heater materials:	
Tube	Multimet N-155
Cylinder and regenerator housings	Haynes Stellite HS-31
Preheater type	recuperative
Preheater material	310 stainless steel sheet
Number of regenerator/coolers per engine cylinder	2
Regenerator material	304 stainless steel wire mesh gauze
Piston rod seal type	sliding (pumping Leningrader)
Piston rod seal and piston ring material	RULON LD (filled PTFE)

[a]Mean cycle pressure, 15 MPa; heater temperature, 720° C; cooler temperature, 50° C.
[b]Including gas in storage bottle.
[c]Controlled by Bosch K-Jetronic continuous fuel injection system.

TABLE II. - P40 START-STOP SEQUENCES

(a) Automatic Start Sequence

1. Key switch from off to power on - turns on electronics
2. Key switch to auto start (spring return to power on): Starting up electric motor drives combustion air blower, atomizing air compressor, and hydraulic pump Electric fuel pump starts Air throttle moves to start position Gas supplied, if needed, to produce proper engine start pressure
3. After 3 sec: Fuel valve opens, ignition on, combustion starts, heater-tube temperature rises
4. Tube temperature ≈600° C, starter motor cranks engine
5. Engine at ≈500 rpm, starter motor stops cranking
6. Engine at ≈700 rpm, starting up electric motor stops (engine alone drives auxiliaries)
7. Engine at ≈900 rpm, power control system activated, fast idling speed remains until exhaust gas temperature exceeds 160° C
8. Rear tube temperature up to 600° C, recommended drive lamp out

(b) Automatic Stop Sequence

1. Key switch to off - fuel stops, ignition off
2. Power control valve to dump-short-circuit position, engine runs at idling speed
3. Engine runs on remaining heat
4. Engine stops, electric after-cooling water pump on
5. After-cooling timer out, electronics off

TABLE III. - P40 INSTRUMENTATION SUPPLIED BY UNITED STIRLING AND NASA SYMBOL

Heater tube wall temperature - 8 control thermocouples	THTMAX
Heater tube wall temperature - 16 data thermocouples	THT01-16
Exhaust gas temperature entering preheater - 4 thermocouples	USSPHT
Air throttle position	.ATPOS
Engine cooling water outlet temperature	.USSWT
Engine oil outlet temperature	TOILRT
Engine speed	RPMUSS
Accelerator level/desired engine pressure	ACCLEV
Maximum cycle pressure	.USS28
Pressure before hydrogen compressor	.USS42
Pressure after hydrogen compressor	.USS43
Hydrogen storage tank pressure	.USS17
Power control servovalve position	PCVPOS

TABLE IV. - INSTRUMENTATION INSTALLED ON P40 ENGINE NUMBER 1

(a) Temperature sensing instruments

Symbol	Measurement description	Sensor	Recording range, °C	Full-scale instrument accuracy, °C
TAMB	Test cell ambient temperature	Chromel/Constantan thermocouple	139	±1.2
TAIRIN	Combustion air temperature at flowmeter	↓	↓	↓
TCOMIN	Atomizing air temperature at compressor inlet			
TNOAIR	Atomizing air temperature at fuel nozzle			
TBLOIN	Combustion air temperature at blower inlet			
EGRMT	Exhaust gas temperature at EGR flowmeter	Chromel/Alumel thermocouple	188	
TEGR	Recirculated exhaust gas temperature	Chromel/Constantan thermocouple	208	
TREGR	Blower bypass mixed gas temperature	Chromel/Constantan thermocouple	139	
TPHIN	Combustion air temperature at preheater inlet	Chromel/Constantan thermocouple	139	
TGPAI1	Preheater inlet air temperature	Chromel/Alumel thermocouple	188	
TGPAI2	Preheater inlet air temperature	↓	188	
TGPAI3	Preheater inlet air temperature		188	↓
TGPAO1	Preheater outlet air temperature		1034	±4.0
TGPAO2	Preheater outlet air temperature		↓	↓
TGPAO3	Preheater outlet air temperature			
TGPEI1	Preheater inlet exhaust gas temperature			
TGPEI2				
TGPEI3			▽	↓
TGPEO1	Preheater outlet exhaust gas temperature		547	±2.2
TGPEO2			547	±2.2
TGPEO3			547	±2.2
TGTI	Turbulator inlet gas temperature		1034	±4.0
TWPAI	Preheater wall temperature at air inlet		311	±1.3
TWPAO	Preheater wall temperature at air outlet		1034	±4.0
TWPEI	Preheater wall temperature at exhaust inlet		[a]1371	±5.3
TWPEO	Preheater wall temperature at exhaust outlet		547	±2.2
TWPI1	Preheater inside surface wall temperature		[a]1371	±5.3
TWPI2	↓		[a]1371	±5.3
TWPI3			1034	±4.0
TWPI4			1034	±4.0
TWPI5			1034	±4.0
TWPI6			[a]1371	±5.3
TWPI7			1034	±4.0
TWPI8			1034	±4.0
TWPI9	▽	▽	1034	±4.0

[a]At 52.26 MV.

TABLE IV. - Continued.

(a) Continued.

Symbol	Measurement description	Sensor	Recording range, °C	Full-scale instrument accuracy, °C
TWPI10	Preheater inside surface wall temperature	Chromel/Alumel thermocouple	1034	±4.0
TWPI11	Preheater inside surface wall temperature			
TWPO1	Preheater outside surface wall temperature			
TWPO2				
TWPO3				
TWPO4				
TWPO5				
TWPO6				
TWPO7				
TWPO8				
TWPO9				
TWPSP	Preheater wall temperature at ignitor			
TWPBP	Preheater wall temperature at base plate			
TWIC1	Heater-head insulation cover wall temperature		[a]1371	±5.3
TWIC2			1034	±4.0
TWIC3				
TWIC4				
TWIC5				
TWCS	Ceramic stone wall temperature		[a]1371	±5.3
TWB1	Combustor housing wall temperature			
TWB2	Combustor housing wall temperature			
TGBT1	Combustion gas temperature between tubes			
TGTE1	Combustion gas temperature after tubes		1034	±4.0
TGTE2				
TGTE3				
TGTE4				
TGTE5				
TGTE6[b]				
TGTE7				
TGTE8[b]				
TGTE9				
TGTE10[b]				
TGTE11				
TGTE12[b]				
TGTE13				
TGTE14				
USSPHT			1000	----
TEXHR	Preheater exhaust temperature from right outlet	Chromel/Constantan thermocouple	338	±1.4
TEXHL	Preheater exhaust temperature from left outlet	Chromel/Constantan thermocouple	338	±1.4
TSTACK	Exhaust stack gas temperature	Chromel/Constantan thermocouple	338	±1.4

[a]At 52.26 MV.
[b]Used for control system preheater temperature (USSPHT).

TABLE IV. - Continued.

(a) Continued.

Symbol	Measurement description	Sensor	Recording range, °C	Full-scale instrument accuracy, °C
THT1	Heater-tube wall temperature	Chromel/Alumel thermocouple	1034	±4.0
THT2	↓	↓	↓	↓
THT3				
THT4				
THT5				
THT6				
THT7				
THT8				
THT9				
THT10				
THT11				
THT12				
THT13				
THT14				
THT15				
THT16				
THT1N				
THT1C				
THT2N				
THT2C				
THT3N				
THT3C				
THT4N				
THT4C	↓		↓	↓
THTMAX	Maximum control heater-tube wall temperature		1000	----
TES1	Expansion space gas temperature - cycle 1		1034	±4.0
TES2	Expansion space gas temperature - cycle 2		↓	↓
TES3	Expansion space gas temperature - cycle 3			
TES4	Expansion space gas temperature - cycle 4			
TCS1	Compression space gas temperature - cycle 1		188	±1.2
TCS2	Compression space gas temperature - cycle 2		↓	↓
TCS3	Compression space gas temperature - cycle 3			
TCS4	Compression space gas temperature - cycle 4			
TWC1	Cylinder housing wall temperature		1034	±4.0
TWC2	↓		↓	↓
TWC3				
TWC4				
TWC5				
TWC6				
TWC7			547	±2.2
TWC8			1034	±4.0
TWC9			1034	±4.0
TWC10	↓	↓	547	±2.2

TABLE IV. - Continued.

(a) Concluded.

Symbol	Measurement description	Sensor	Recording range, °C	Full-scale instrument accuracy, °C
TWC11	Cylinder housing wall temperature	Chromel/Alumel thermocouple	547	±2.2
TWC12	Cylinder housing wall temperature	↓	1034	±4.0
TWIR1	Inner regenerator housing wall temperature	↓	1034	±4.0
TWIR2	↓	↓	1034	±4.0
TWIR3	↓	↓	547	±2.2
TWIR4	↓	↓	547	±2.2
TWIR5	↓	↓	1034	±4.0
TWOR1	Outer regenerator housing wall temperature	↓	↓	↓
TWOR2	↓	↓	↓	↓
TWOR3	↓	↓	↓	↓
TWOR4	↓	↓	547	±2.2
TWOR5	↓	↓	1034	±4.0
TCWIN	Engine cooling water inlet temperature	Chromel/Constantan thermocouple	139	±1.2
USSWT	Engine cooling water outlet temperature	Iron/Constantan thermocouple	100	----
TDLCW	Engine cooling water differential temperature	Copper/Constantan thermocouple	18	±.5
TCTW	Cooling tower water temperature	Chromel/Constantan thermocouple	139	±1.2
TOILIN	Engine oil inlet temperature	Chromel/Constantan thermocouple	139	±1.2
TOILRT	Engine oil outlet temperature	Resistance temperature detector	100	----
TDELO	Engine oil differential temperature	Copper/Constantan thermocouple	9	±.5

TABLE IV. - Continued.

(b) Pressure sensing instruments

Symbol	Measurement description	Sensor	Recording range	Full-scale instrument accuracy
PAIRIN	Combustion air pressure at flowmeter	Strain-gage pressure transducer	12.6 kPa	±0.11 kPa
PNOAIR	Atomizing air pressure at fuel nozzle		115 kPa	±.49 kPa
PFNOZ	Fuel pressure at fuel nozzle		140 kPa	±.60 kPa
PBLOIN	Combustion air pressure at blower inlet		6.9 kPa	±.06 kPa
PBLOUT	Combustion air pressure at blower outlet		12.0 kPa	±.10 kPa
PPHIN	Combustion air pressure at preheater inlet		34.5 kPa	±.29 kPa
PPHAI	Preheater inlet air pressure		22.7 kPa	±.19 kPa
PPHAO	Preheater outlet air pressure		23.5 kPa	±.20 kPa
PPHEI	Preheater inlet exhaust gas pressure		24.0 kPa	±.20 kPa
PPHEO	Preheater outlet exhaust gas pressure		24.1 kPa	±.20 kPa
PTI	Combustion air pressure at turbulator inlet		24.1 kPa	±.20 kPa
PCOMB	Combustion chamber pressure		34.5 kPa	±.29 kPa
PBT	Combustion gas pressure between tubes		23.5 kPa	±.20 kPa
PAT	Combustion gas pressure after tubes		23.4 kPa	±.20 kPa
PEXHR	Preheater exhaust pressure from right outlet		6.9 kPa	±.06 kPa
PEXHL	Preheater exhaust pressure from left outlet		6.9 kPa	±.06 kPa
PSTACK	Exhaust stack gas pressure		6.8 kPa	±.06 kPa
EGRMIP	Exhaust gas pressure at EGR flowmeter		13.1 kPa	±.11 kPa
PH2SUP	Working gas supply pressure		17.2 MPa	±.07 MPa
USS17	Working gas supply pressure		20 MPa	--------
ACCLEV	Accelerator level/desired engine pressure		20 MPa	--------
HPSUP	Supply pressure from power control valve		27.6 MPa	±.12 MPa
MAXCP	Maximum compression space cycle pressure		22.2 MPa	±.10 MPa
USS28	Maximum compression space cycle pressure		20 MPa	--------
MINCP	Minimum compression space cycle pressure		18.3 MPa	±.08 MPa
PSEAL	Piston rod seal housing pressure		22.9 MPa	±.10 MPa
PMEAN1	Mean compression space pressure - cycle 1		23.1 MPa	±.10 MPa
PMEAN2	Mean compression space pressure - cycle 2		23.2 MPa	±.10 MPa
PMEAN3	Mean compression space pressure - cycle 3		21.4 MPa	±.09 MPa
PMEAN4	Mean compression space pressure - cycle 4		23.2 MPa	±.10 MPa

TABLE IV. - Continued.

(b) Concluded.

Symbol	Measurement description	Sensor	Recording range	Full-scale instrument accuracy
PCS1	Compression space dynamic pressure - cycle 1	Strain-gage pressure transducer	20.7 MPa	±0.21 MPa
PCS2	Compression space dynamic pressure - cycle 2			
PCS3	Compression space dynamic pressure - cycle 3			
PCS4	Compression space dynamic pressure - cycle 4			
PES1	Expansion space dynamic pressure - cycle 1			
PES2	Expansion space dynamic pressure - cycle 2			
PES3	Expansion space dynamic pressure - cycle 3			
PES4	Expansion space dynamic pressure - cycle 4			
PH2BC	Working gas pressure before compressor		26.9 MPa	±.12 MPa
USS42	Working gas pressure before compressor		20 MPa	--------
PH2AC	Working gas pressure after compressor		27 MPa	±.12 MPa
USS43	Working gas pressure after compressor		20 MPa	--------
IMEPC1	Compression space IMEP - cycle 1	IMEP measurement system electronics	5 MPa	±.05 MPa
IMEPC2	Compression space IMEP - cycle 2			
IMEPC3	Compression space IMEP - cycle 3			
IMEPC4	Compression space IMEP - cycle 4			
IMEPE1	Expansion space IMEP - cycle 1			
IMEPE2	Expansion space IMEP - cycle 2			
IMEPE3	Expansion space IMEP - cycle 3			
IMEPE4	Expansion space IMEP - cycle 4			
PCWIN	Engine cooling water inlet pressure	Strain gage pressure transducer	114 kPa	±.49 kPa
PDELCW	Engine cooling water differential pressure		57.5 kPa	±.49 kPa
DYH2OP	Dynamometer cooling water pressure		758 kPa	±3.3 kPa
POIL	Engine oil pressure		766 kPa	±3.3 kPa
PN2CV	Nitrogen pressure for crankcase vent		115 kPa	±.49 kPa
PCRANK	Crankcase pressure		61.2 kPa	±.52 kPa

TABLE IV. - Continued.

(c) Miscellaneous sensors

Symbol	Measurement description	Sensor	Recording range	Full-scale instrument accuracy
FFLO	Fuel mass flow rate	Flotron mass flowmeter	6.3 g/s	±0.03 g/s
NAFLO	Atomizing air mass flow rate	Hastings mass flowmeter	2.2 g/s	±0.02 g/s
CAFLO	Combustion air flow rate	Turbine flow meter	83.7 l/s	±0.9 l/s
EGRFLW	Exhaust gas recirculation flow rate	Vortex shedding flow meter	94.4 l/s	±0.9 l/s
CWFLOC	Engine cooling water flow rate	Turbine flowmeter	5.0 l/s	±0.03 l/s
OILFLO	Engine lubrication oil flow rate	Turbine flowmeter	15.8 l/m	±0.16 l/m
PCVPOS	Power control valve position	Potentiometer	±100%	----------
TORQUE	Engine torque from dynamometer	Strain gage load cell	203 N·m	±2 N·m
RPM1	Engine speed	Magnetic speed pickup	4200 rpm	±10 rpm
RPM2	Engine speed from dynamometer	Magnetic speed pickup	7500 rpm	±19 rpm
RPMUSS	Engine speed	Magnetic speed pickup	5000 rpm	----------
HPDYN	Engine power from dynamometer	Dynamometer electronics	60 kW	±0.6 kW
MEPMRK	IMEP cycle marker from MEIS	IMEP measurement system electronics	1 - 4	----------
ALTV	Alternator voltage	Voltage divider	15 V	±0.04 V
ALTI	Alternator current	Current shunt	80 A	±0.2 A
VX1	Engine horizontal vibration	Accelerometer	38 mm/s	±2 mm/s
VY1	Engine vertical vibration	Accelerometer	38 mm/s	±2 mm/s
ANGLE	Drive shaft rotational position	Shaft angle encoder	360°	±0.2°
DEGREE	Drive shaft rotational position (10° pulses)	Shaft angle encoder	360°	±0.2°
HUMID	Test cell relative humidity	Impedance type	100%	±5%
RPMBLO	Combustion air blower speed	Magnetic speed pickup	8000 rpm	±20 rpm
ATPOS	Air throttle position	Potentiometer	100%	----------
EGRMRK	EGR solenoid valve position	Switch	Open/closed	----------
STANO	Emission sampling station number	Selector switch	1 - 5	----------
CORNG	Carbon monoxide analyzer range	Selector switch	100, 500, 2500 ppm	----------

TABLE IV. - Continued.

(c) Concluded.

Symbol	Measurement description	Sensor	Recording range	Full-scale instrument accuracy
COSIG	Carbon monoxide analyzer signal	Nondispersive infrared detector	100, 500, 2500 ppm	±5, ±25, ±125 ppm
CO2RNG	Carbon dioxide analyzer range	Selector switch	5, 10, 20%	----------
CO2SIG	Carbon dioxide analyzer signal	Nondispersive infrared detector	5, 10, 20%	±0.25, ±0.5, ±1%
NOXRNG	Nitrogen oxide analyzer range	Selector switch	1 - 10 000 ppm	----------
NOXSIG	Nitrogen oxide analyzer signal	Chemiluminescence detector	1 - 10 000 ppm	±0.05 - ±500 ppm
HCMP''G	Hydrocarbon analyzer range multiplier	Selector switch	0.2, 1.0, 10.0	----------
HCRNG	Hydrocarbon analyzer range	Selector switch	5 - 10 000 ppm	----------
HCSIG	Hydrocarbon analyzer signal	Flame ionization detector	5 - 10 000 ppm	±0.25 - ±500 ppm
O2RNG	Oxygen analyzer range	Selector switch	1, 5, 10, 25%	----------
O2SIG	Oxygen analyzer signal	Paramagnetic detector	1, 5, 10, 25%	±0.05, ±0.25, ±0.5, 1.25%

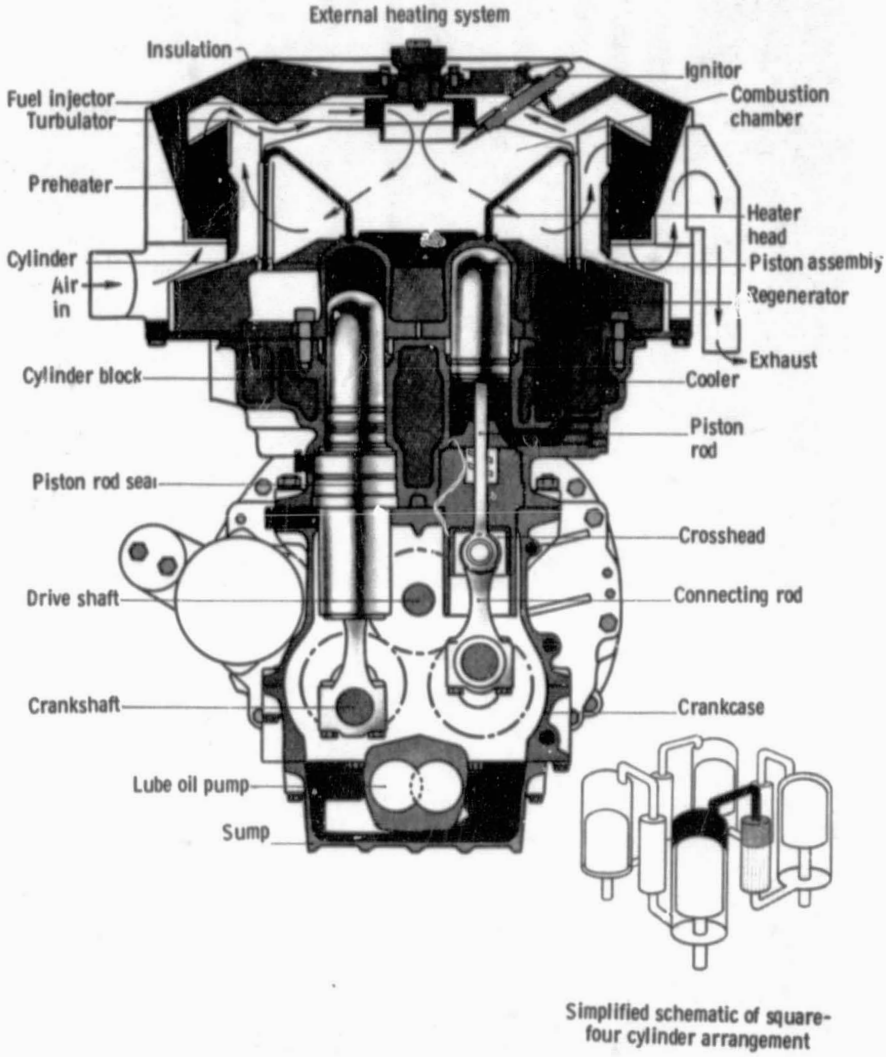

Figure 1. - P40 Stirling engine cross section.

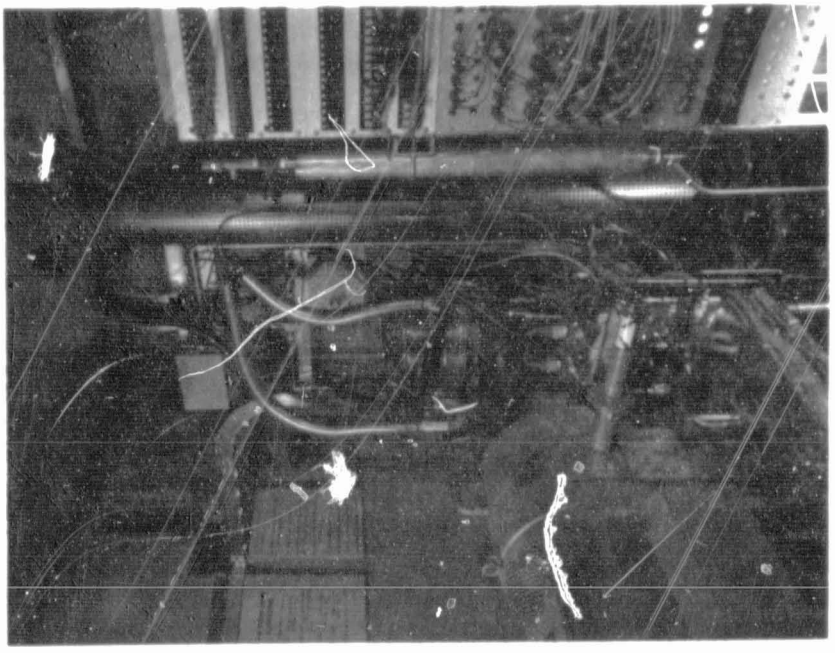

(b) Rear view.

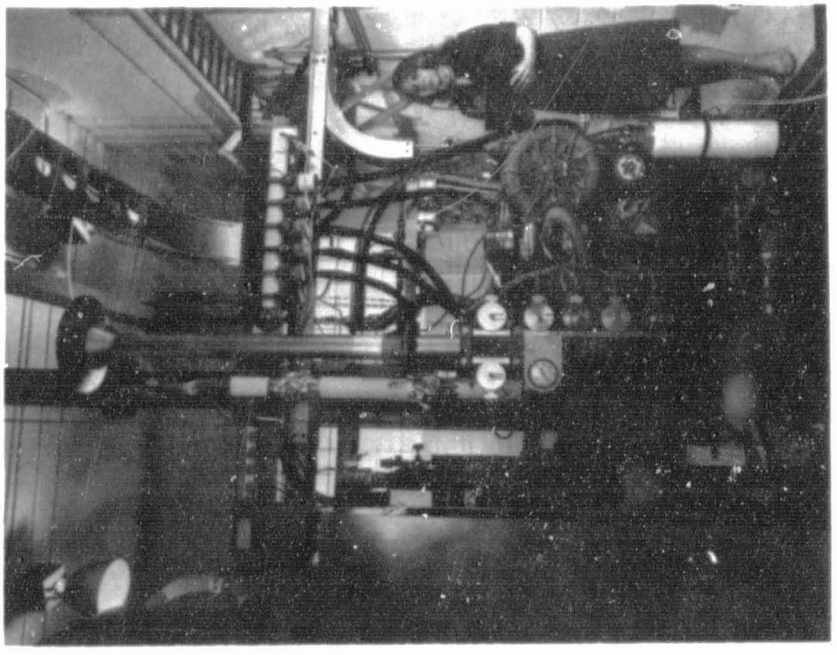

(a) Front view.

Figure 2. - P40 installed in NASA test cell.

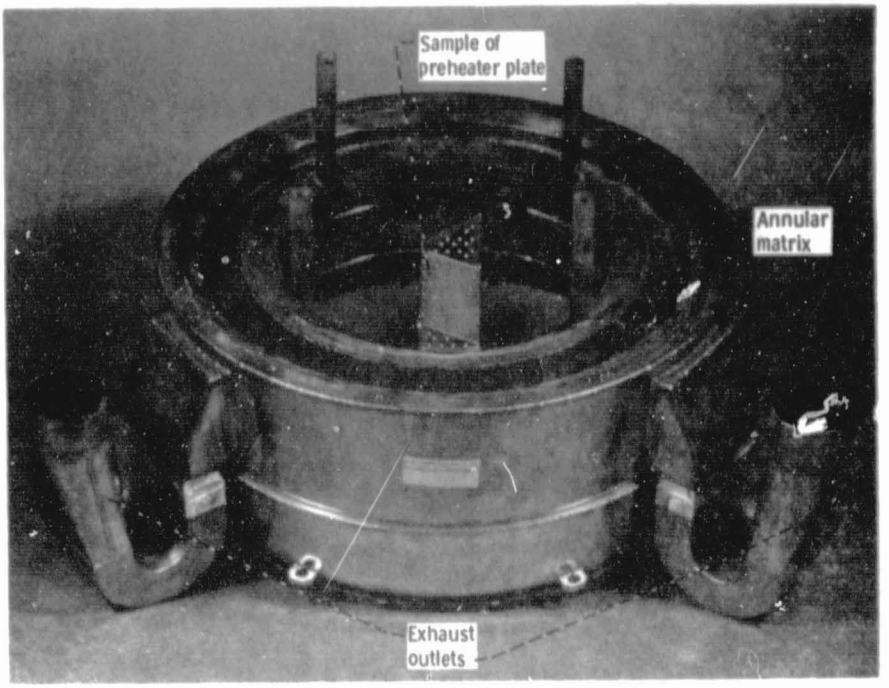

Figure 3. - P40 preheater assembly.

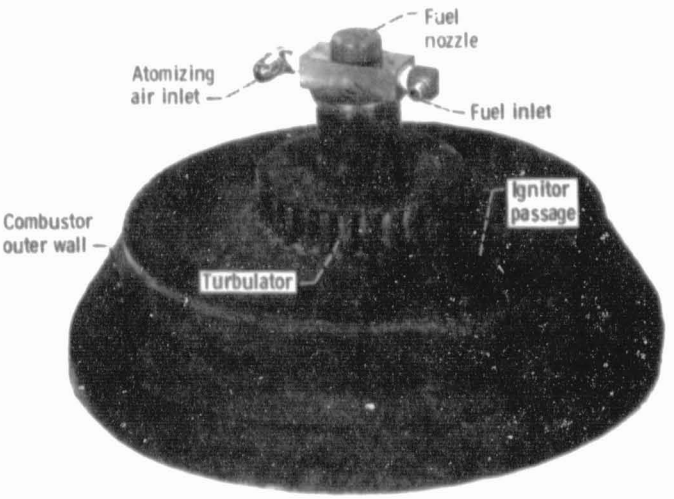

Figure 4. - P40 combustor/fuel nozzle assembly.

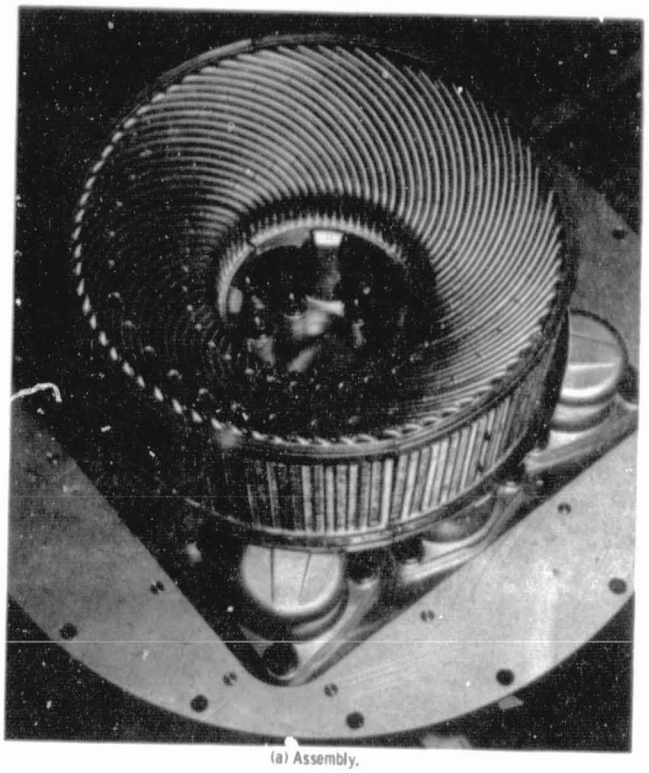

(a) Assembly.

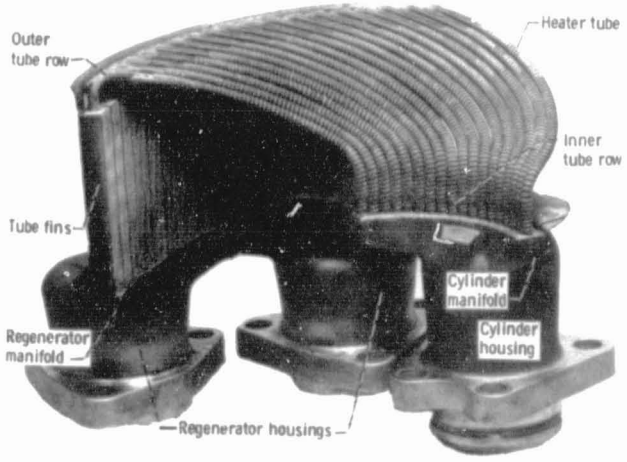

(b) Quadrant.

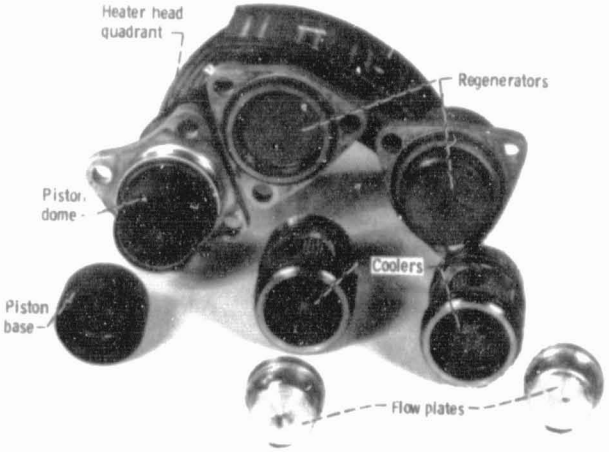

(c) Quadrant components.

Figure 5. - P40 Heater head.

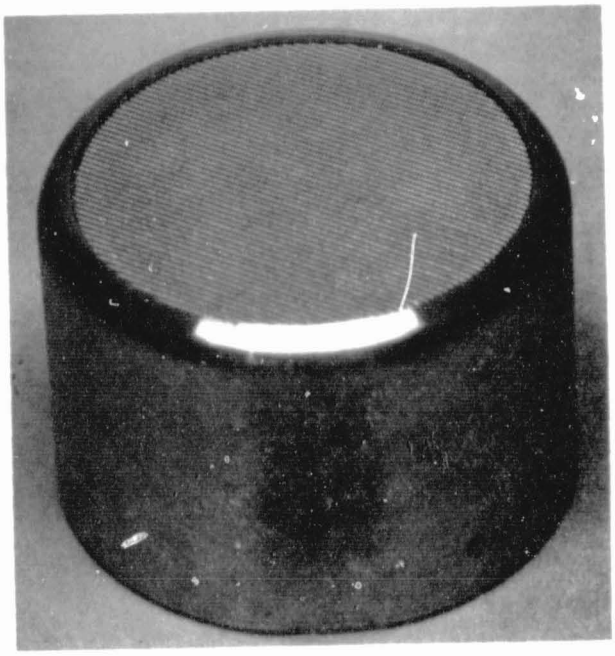

Figure 6. - P4C regenerator.

Figure 7. - P40 cooler.

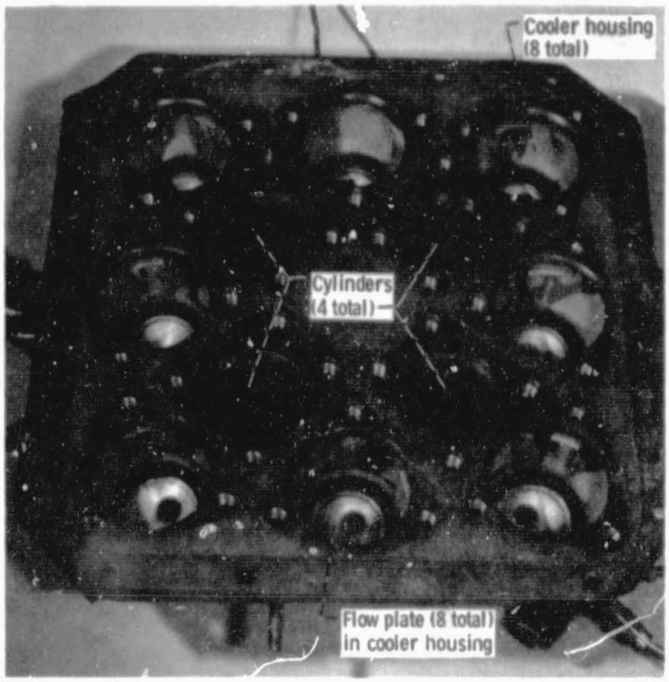

Figure 8. - P40 cylinder block.

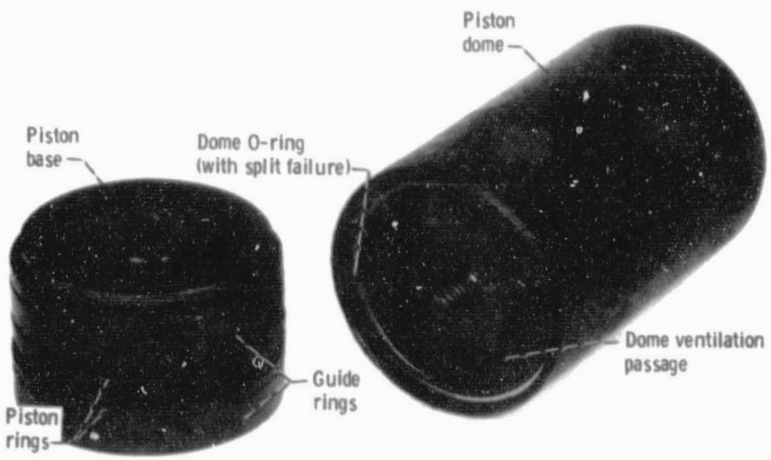

Figure 9. - P40 piston assembly.

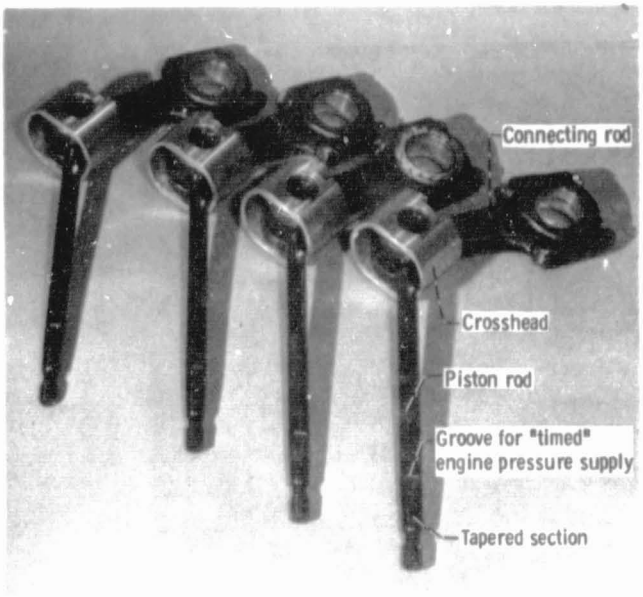

Figure 10. - P40 piston rod, crosshead, and connecting rod assemblies.

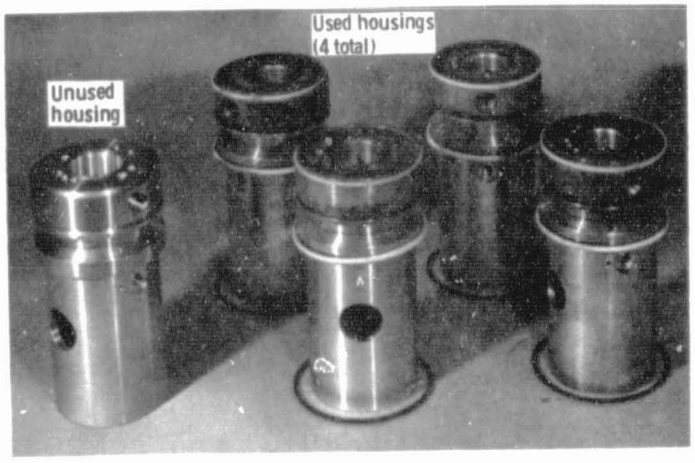

(a) Housing.

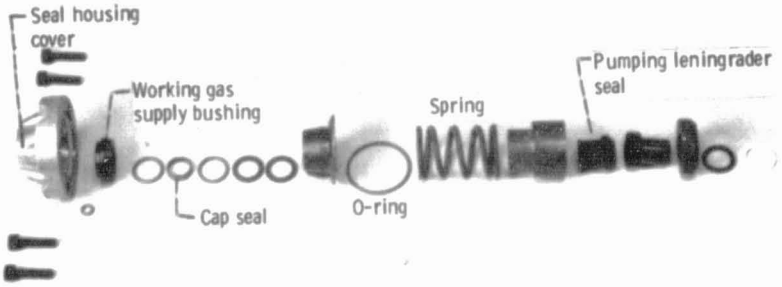

(b) Assembly stackup.

Figure 11. - P40 piston rod seal.

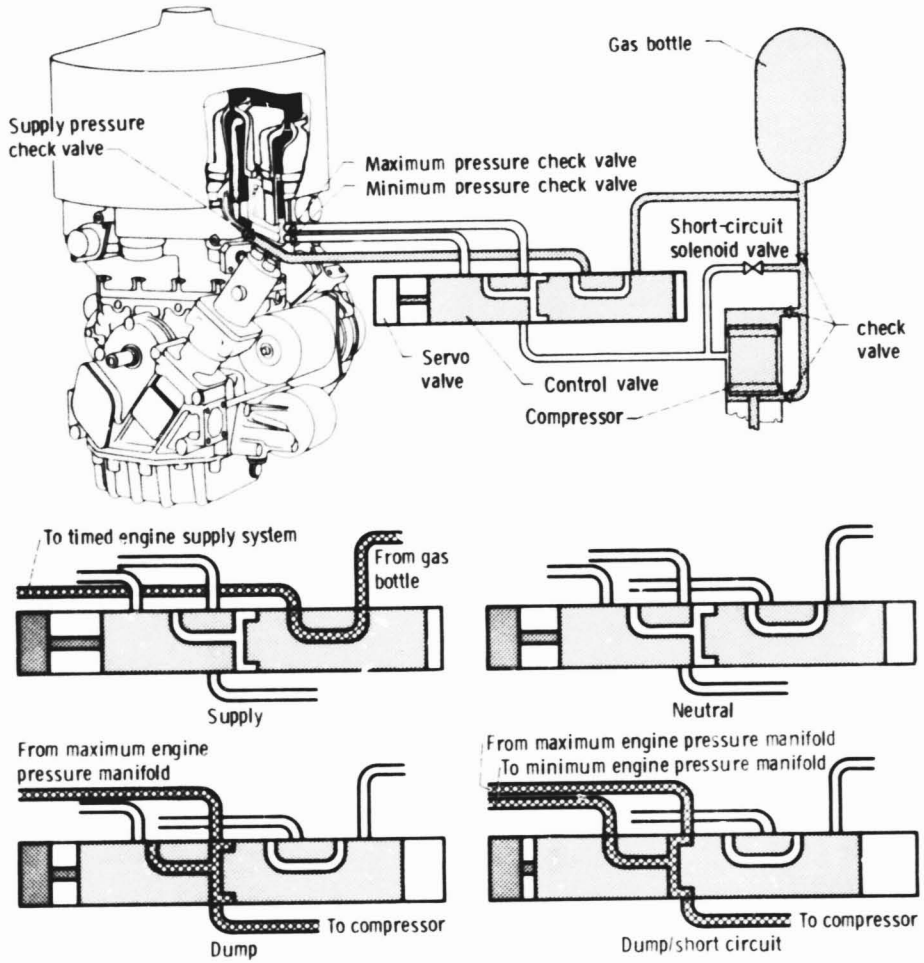

Figure 12. - P40 power control system schematic.

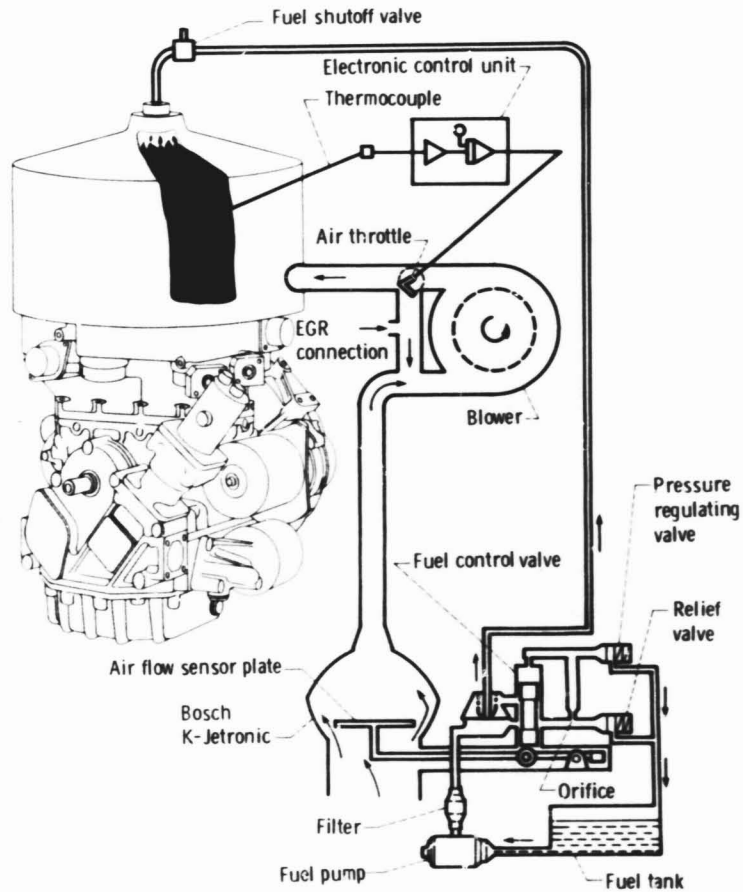

Figure 13. - P40 temperature and air-fuel control system schematic.

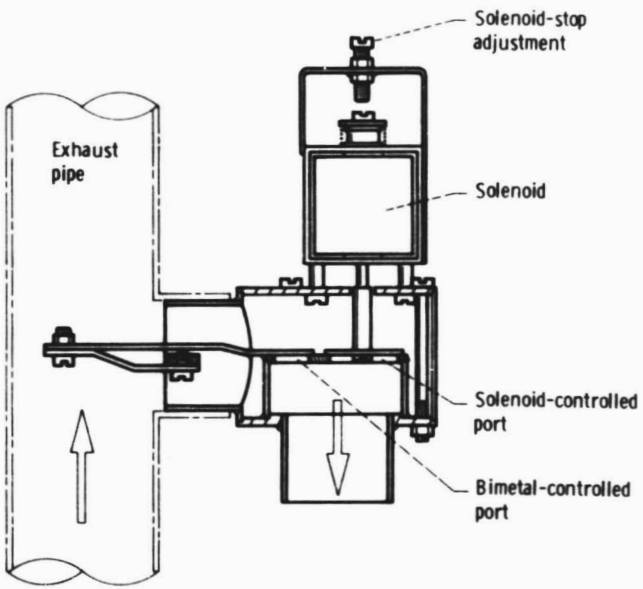

Figure 14. - P40 exhaust gas recirculation valve schematic.

Figure 15. - P40 control panel and electronic unit.

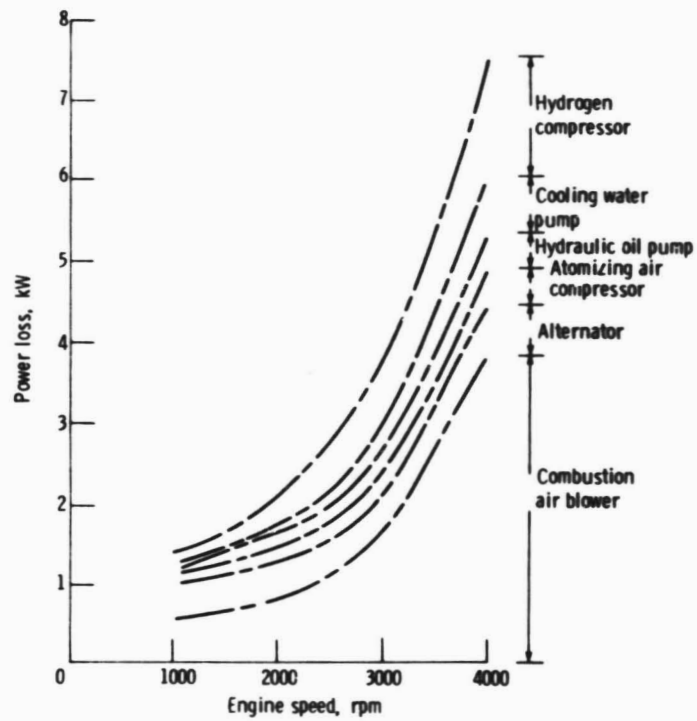

Figure 16. - P40 auxiliaries power consumption at 15 MPa mean cycle pressure.

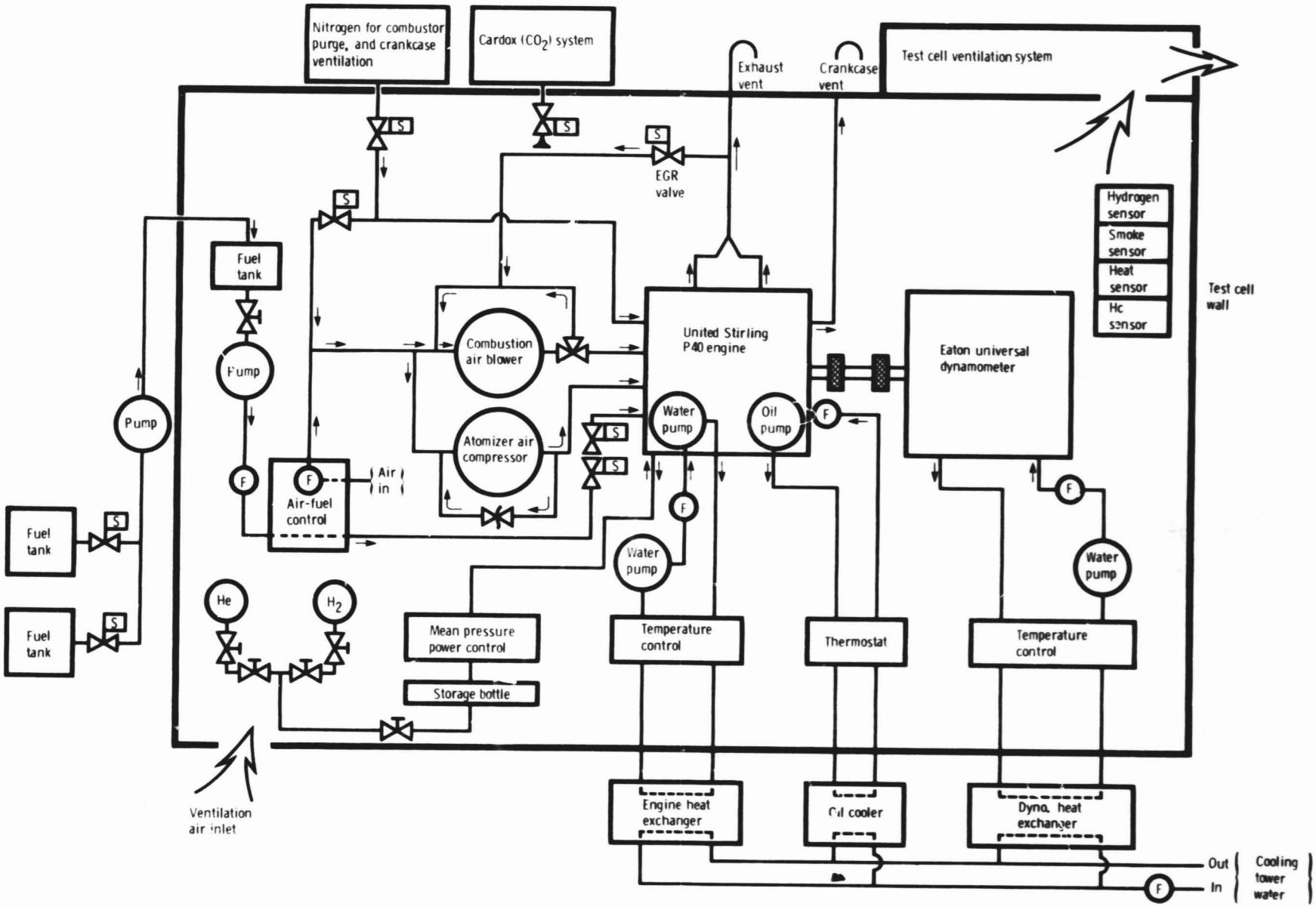

Figure 17. - P40 test facility systems simplified schematic.

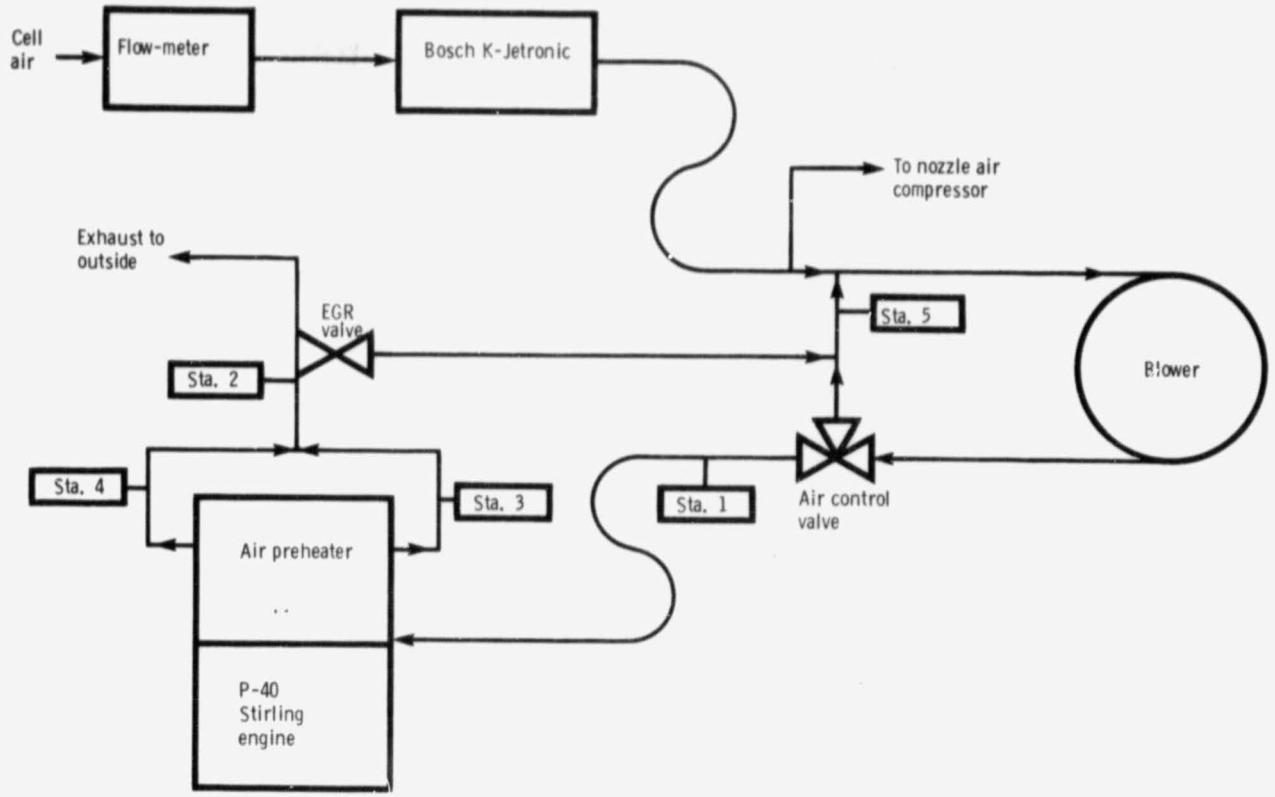

Figure 18. - P-40 combustion system emission sampling stations.

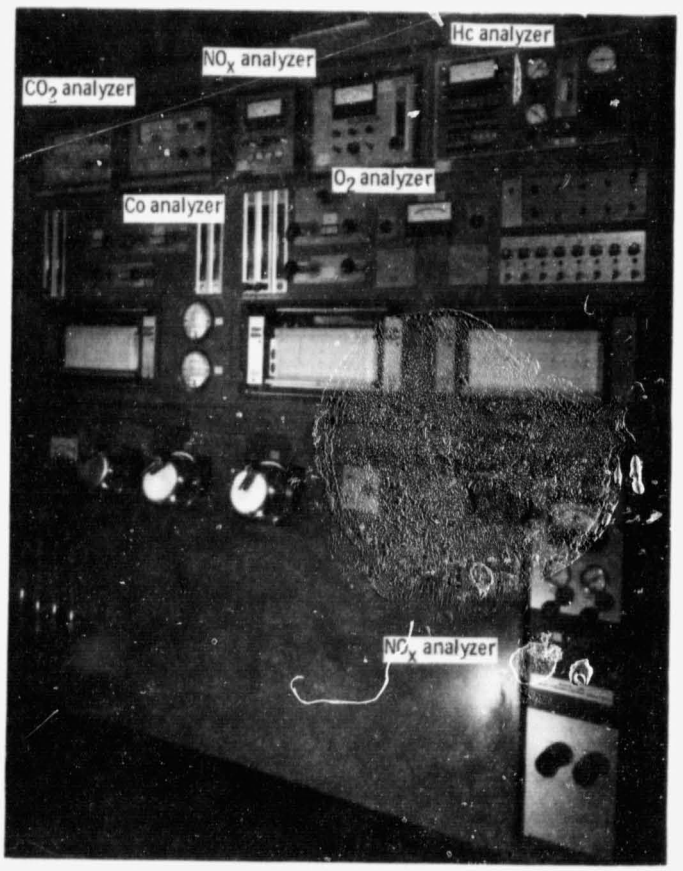

Figure 19. - Exhaust emissions analyzer system.

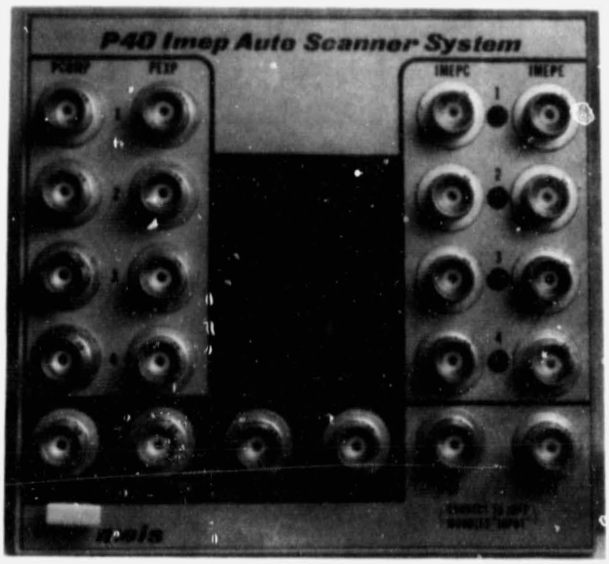

(a) Front view.

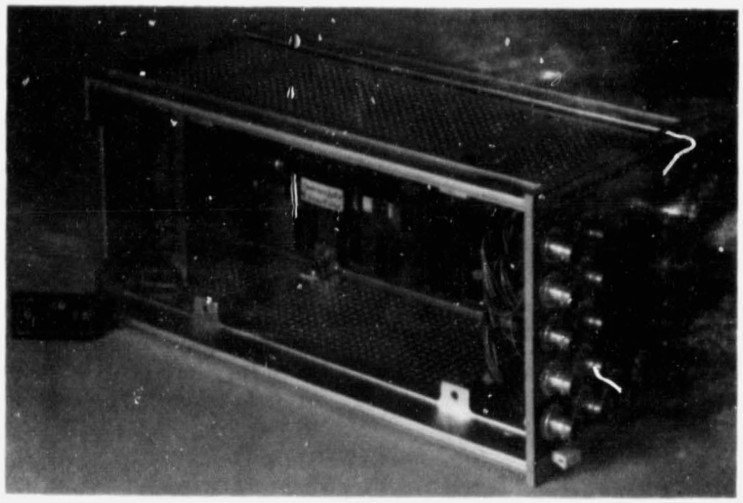

(b) Side view.

Figure 20. - P40 IMEP measurement system electronics.

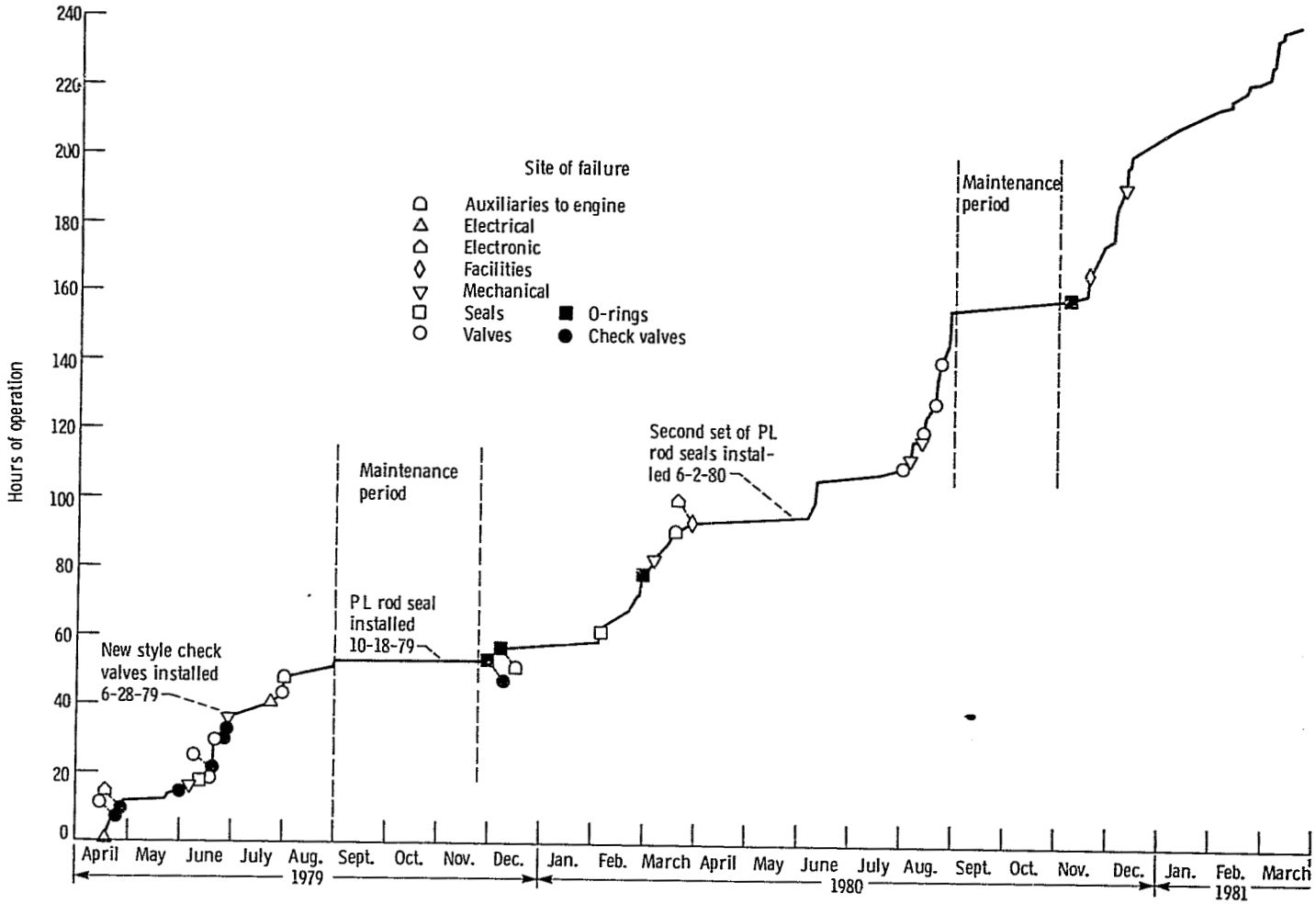

Figure 21. - P40 no. 1 operating history at NASA.

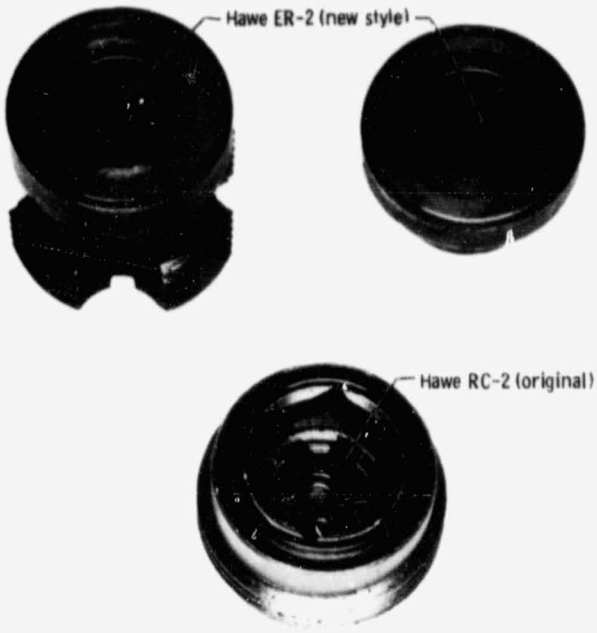

Figure 22. - Mean pressure control system check valves.

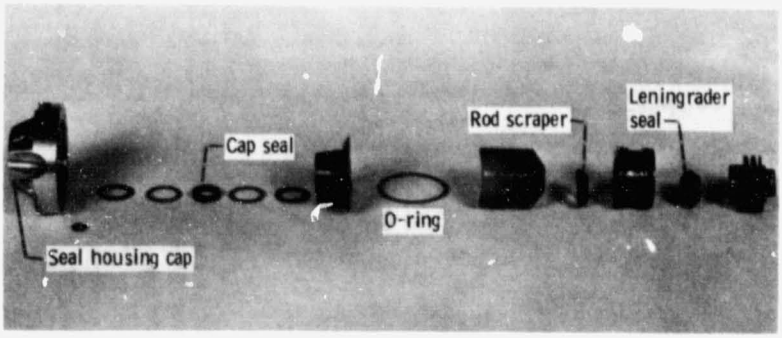

Figure 23. - P40 Leningrader rod seal assembly stackup (original seal used in engine).

Figure 24. - Instrumented P40 heater head quadrant.

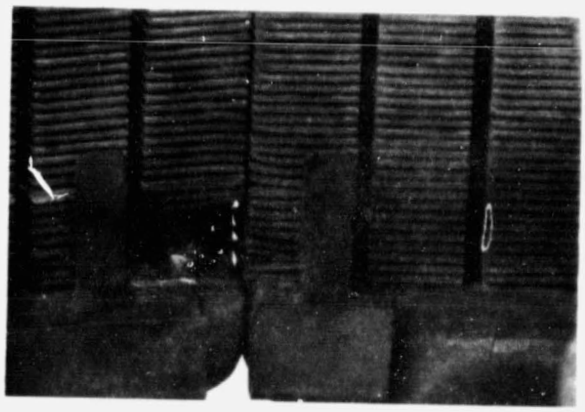

(a) With fins removed.
Figure 25. - Repaired heater tube braze joint.

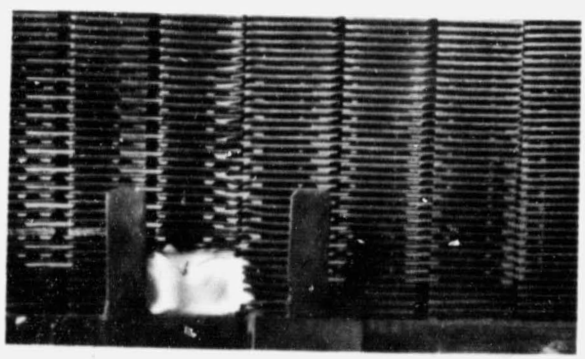

(b) With ceramic filler.
Figure 25. - Concluded.

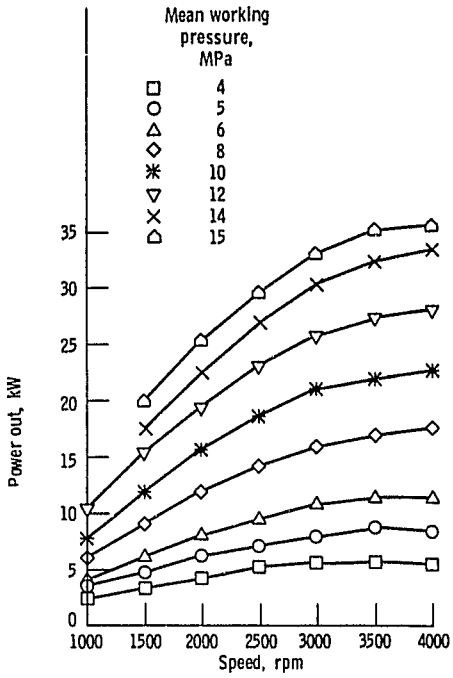

(a) Brake power out versus engine speed.

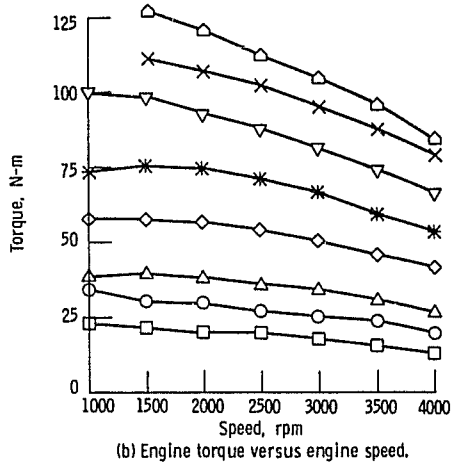

(b) Engine torque versus engine speed.

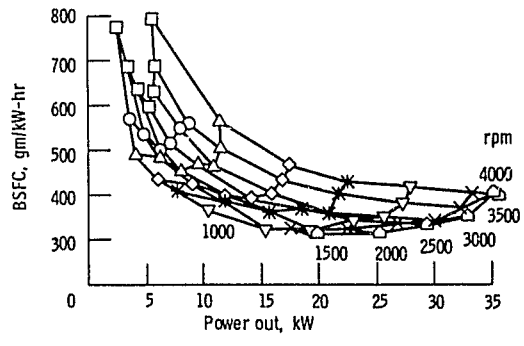

(c) Brake specific fuel consumption versus brake power out.

Figure 26. - Measured engine performance results for hydrogen working gas. Average measured heater tube wall temperature, 720° C; cooling water inlet temperature, 50° C.

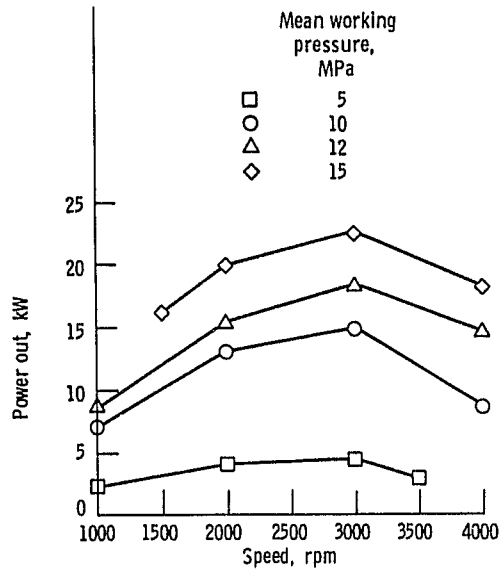

(a) Brake power out versus engine speed.

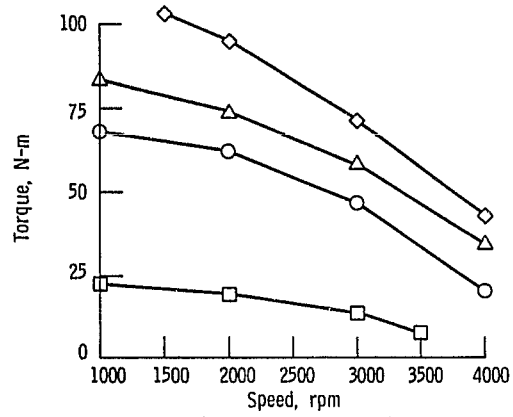

(b) Engine torque versus engine speed.

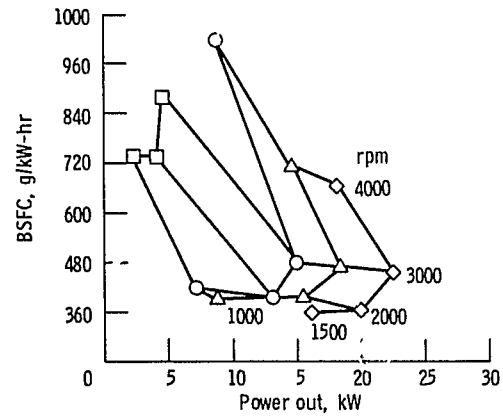

(c) Brake specific fuel consumption versus brake power out.

Figure 27. - Measured engine performance results for helium working gas. Average heater tube wall temperature, 720° C; cooling water inlet temperature, 50° C.

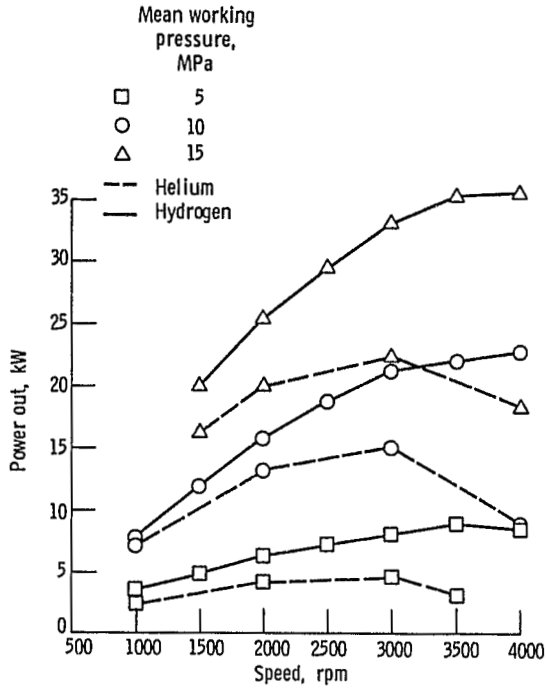

Figure 28. - Hydrogen-helium working gas comparison. Average measured heater tube wall temperature, 720° C; cooling water inlet temperature, 50° C.

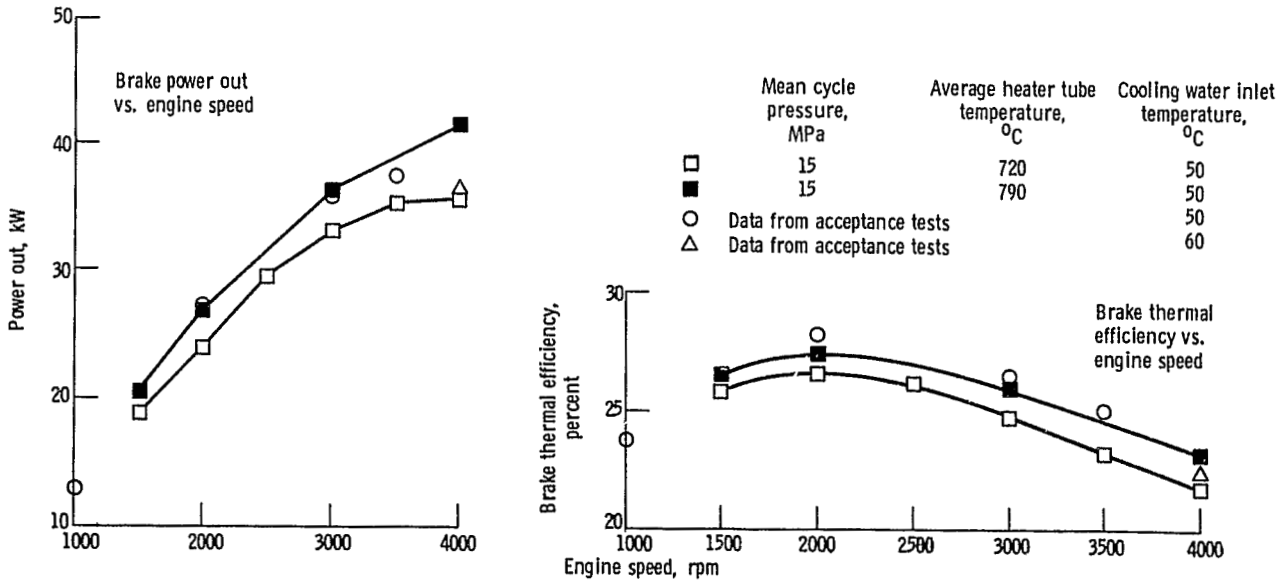

Figure 29. - Engine performance with increased heater tube temperature; working gas, hydrogen.